HARVARD UNIVERSITY

Graduate School of Arts and Sciences

DISSERTATION ACCEPTANCE CERTIFICATE

The undersigned, appointed by the

Harvard John A. Paulson School of Engineering and Applied Sciences
have examined a dissertation entitled:

"The Microbiome of Airborne Particles"

presented by: Rebecca Ariel Stern

Signature _____
Typed name: Professor E. Sunderland

Signature _____
Typed name: Professor S. Wofsy

Signature _____
Typed name: Professor N. Mahmoudi

Signature _____
Typed name: Professor P. Koutrakis

March 19, 2021

The Microbiome of Airborne Particles

A DISSERTATION PRESENTED
BY
REBECCA ARIEL STERN
TO
THE DEPARTMENT OF ENGINEERING SCIENCES

IN PARTIAL FULFILLMENT OF THE REQUIREMENTS
FOR THE DEGREE OF
DOCTOR OF PHILOSOPHY
IN THE SUBJECT OF
ENVIRONMENTAL SCIENCE AND ENGINEERING

HARVARD UNIVERSITY
CAMBRIDGE, MASSACHUSETTS
MARCH 2021

Thesis advisor: Professor Elsie M. Sunderland Rebecca Ariel Stern

The Microbiome of Airborne Particles

Abstract

Airborne microorganisms can strongly influence environmental and human health. However, the airborne microbiome in many locations remains largely uncharacterized. Understanding what microbes are present, where they are located, and how they spread is essential for predicting their presence and function. The transport and spread of airborne microbes is affected by their associations with particles of different sizes. Associations with smaller particles also increases the likelihood that they will penetrate deeply into the lungs and bloodstream. In Chapter 1, I describe the airborne microbiome in the Sahara, a globally important source region for atmospheric dust. Results showed abundant and diverse microbes in all size fractions, including potential pathogens, even on fine particles (≤2.5 μm) that are capable of long-distance transport. In Chapter 2, I explored the presence of severe acute respiratory syndrome coronavirus 2 (SARS-CoV-2), the virus that causes coronavirus disease 2019 (COVID-19), in the air of a Boston hospital. I found airborne SARS-CoV-2 RNA to be present in all particle sizes tested and more prevalent in areas without COVID-19 patients. Presence of the virus on fine particles indicates the ability to remain airborne for extended periods of time and travel farther than six feet. In Chapter 3, I evaluated the location-dependent size distribution of airborne SARS-CoV-2. I conducted a study of SARS-CoV-2 in size-fractionated particles in a healthcare facility in Kuwait. Large particles (≥10 μm) were the predominant source of SARS-CoV-2 in symptomatic patient rooms. By contrast, outside the hospital entrance and in intubated patient rooms, viral RNA was more frequently associated with fine particles. These findings emphasize the importance of universal airborne precautions that protect against fine particles in all locations, including non-COVID-19 wards and outside the hospital. This research demonstrates airborne particles contain an abundant and diverse microbiome with important implications for human health and disease transmission.

Contents

Listing of figures

List of Tables

‘

For James, and his love of walks in the fresh air with all of its microbes.

Acknowledgments

I AM VERY GRATEFUL to many people for their guidance, support, and help throughout my doctoral program. I would like to thank Elsie Sunderland, my advisor, for her wise advice about research, careers, and academia that helped make my Ph.D. experience one that I had always hoped for. I gratefully acknowledge the members of my advisory committee for their direction and advice. I am particularly thankful for the encouragement, guidance, and collaboration of Petros Koutrakis, who made much of these projects possible. I thank Nagissa Mahmoudi for her wonderful mentorship and help with microbiology. I gratefully acknowledge Steve Wofsy for teaching me about atmospheric science and guiding me in preparation for the field work.

I feel fortunate to have met and worked with many wonderful people along the way to this destination. Mike Wolfson and Steve Ferguson taught me so much about the compact cascade impactor. I thank Amina Schartup for her guidance and help during fieldwork and for a life-changing trip to Mali. My thanks to Bruce Daube for teaching me about sampling design and the essentials of aerosol sampling.

My path to graduate school would not have occurred without the guidance of my undergraduate advisor, John Wargo, who helped me find my passion for environmental research. I am grateful to Laura Diaz Anadon and Venky Narayanamurti for helping me and encouraging me and to pursue the Ph.D. path. I wish to thank the members of the Sunderland Lab, Earth and Planetary Sciences Department, Microbial Sciences Institute, and Engineering and Applied Sciences department for being a cornerstone to my wonderful experience as a Ph.D. student. I am grateful for the contributions and support from: Prentiss Balcom, Bocary Traore, Marco Martins, Ali Al-Hemoud, Barrak Alahmad, Joy Lawrence, and Caroline Buckee. The research in this thesis was supported, in part, by funding from the Star-Friedman Challenge for Promising Scientific Research, the U.S. Environmental Protection Agency, and Kuwait Institute for Scientific Research.

Finally, I would like to thank my wonderful family. I am thankful for my parents and brothers for their endless love and motivation. I am particularly grateful to my husband, Kevin, for his unwavering support and humor, which made the completion of this project possible.

0

Introduction

Microorganisms (microbes) are ubiquitous in the air we breathe.[75] Some of these microbes are beneficial and others are harmful.[122] Now more than ever, in the face of global pandemics and interconnectedness, it is imperative to predict how microbes spread through the air. To do so, we must understand what microbes are present in the atmosphere, where they are located, and how they are transported.

Our understanding of the composition, diversity, and abundance of airborne microbes is limited.

Advancements in aerobiology have historically been overshadowed by research focused on more visible agents of disease including insects and contaminated food and water.[62] The atmosphere is the environmental frontier least explored by microbiologists.[109] In addition, until recently, our ability to identify and characterize microbes was limited to the use of culture-based methods. However, less than 1% of environmental microbes are culturable.[153,45,56] Advances in nucleic acid-based technologies such as polymerase chain reaction (PCR), next generation sequencing, and whole-genome shotgun sequencing have allowed researchers to begin to more fully characterize the complete diversity of microbes – estimated to be over 1 trillion microbial species, with over 99.99% of them still to be discovered.[93]

Recent studies harnessing these new technologies have shown that airborne microbes are abundant and diverse, particularly under high-dust conditions, in the Mediterannean[123], Europe[104], USA[20,53], and Asia[27,76,95]. However, the airborne microbiome in other parts of the world remains largely uncharacterized. Air concentrations of bacteria and viruses are estimated to be on the order of approximately 10^6 particles/m^3 outdoors, and approximately 10^5 particles/m^3 indoors.[125] Furthermore, the composition of the airborne microbiome community dictates its functions. Diversity of the microbiome affects its resilience to environmental stress and foreign invaders.[14] Airborne bacteria, for instance, may have diversity comparable to that of soil.[55]

In terms of pathogenic potential, diseases in marine animals[56,168], livestock[30], insects[158], and crops[88,121,18,23] have been linked to the airborne spread of microbial agents. For example, the 1967 outbreak of foot-and-mouth disease in the United Kingdom was traced to long-distance airborne spread[106]. Yet little is known about the long-distance transport of human pathogens in the atmosphere. Over shorter distances, a number of diseases are transmitted via aerosols, including tuberculosis[133], chickenpox[4], and measles.[131] The mode of disease transmission, such as aerosols, is an important factor dictating the severity of illness for many infections.[148]

The impact of airborne microbes does not depend only on the particular taxa present and their

properties (e.g., abundance, antibiotic resistance), but also on their associated particle size. Microbes with smaller particles remain airborne for longer periods of time, penetrate deeper into the lungs, and can be more likely to cause severe infection. [150,112,148] The particle size distribution of airborne microbes is a critical feature dictating their potential for long-distance transport and health effects.

This dissertation investigates three key components of understanding airborne microbial transmission: (1) What microbes are present in indoor and outdoor air; (2) Where the microbes are located in different airborne contexts; and (3) How the microbes spread with particles of different sizes. I used a compact cascade impactor custom-built by the Environmental Chemistry Laboratory at the Harvard T.H. Chan School of Public Health to collect samples of airborne microbes in distinct size fractions. In Chapter 1 [147], I used next generation sequencing to characterize the airborne microbiome in Mali, West Africa, a global source region for atmospheric dust. I examined the effects of particle size on microbial composition and evaluated the presence of potential pathogens. Chapter 2 [146] addressed the Coronavirus Disease 2019 (COVID-19) pandemic with a focus on indoor locations and particle sizes carrying severe acute respiratory syndrome coronavirus 2 (SARS-CoV-2), the virus that causes COVID-19, in a Boston hospital. In Chapter 3 [145], I present one of the most comprehensive studies of size-differentiated airborne SARS-CoV-2 to date, with both indoor and outdoor sampling locations, at a healthcare facility in Kuwait.

The airborne microbiome may likely have a greater influence on our lives in coming years. Increased desertification and dust events, including in the Sahara, due to present and future climate change are expected to cause increased global circulation of airborne dust, which is a known vector for airborne microbes. [149] Airborne biological warfare remains a threat to global security. [12] Pandemics caused by airborne transmission of pathogens are of foremost concern, particularly in today's interconnected world. [51]

The wind had been for twenty-four hours previously E.N.E., and hence, from the position of the ship, the dust probably came from the coast of Africa...The dust collected on the Beagle was excessively fine-grained, and of a red-dish brown colour... it is in considerable part composed of Infusoria, including no less than sixty-seven different forms.

Charles Darwin, 1845

1

The Microbiome of Size-Fractionated Airborne Particles from the Sahara Region

Reproduced with permission from: Stern, R.A., Mahmoudi, N., Buckee, C.O., Schartup, A.T., Koutrakis, P., Ferguson, S.T., Wolfson, J.M., Wofsy, S.C., Daube, B.C. and Sunderland, E.M., 2021. The Microbiome of Size-Fractionated Airborne Particles from the Sahara Region. *Environmental Science and Technology*, 55(3), pp.1487-1496.

Atmospheric dust is known to harbor diverse microbial communities.[64,80] When transported over long distances, airborne microbes can affect human health, agriculture, and ecosystem function thousands of kilometers away from source regions.[101,83,63,65,61] The Sahara Desert is the largest global dust source, particularly during the dry Harmattan winds season between late November and mid-March.[105] Frequency of dust events and total dust emissions have increased in the Sahara due to changes in land management practices since the 1960s and desertification.[105] Large quantities (10^9 tonnes per year) of atmospheric dust particles have been transported from the Sahara to the Mediterranean, Europe, and the Americas, among other regions.[35,110] Average wintertime atmospheric dust concentrations in Saharan countries such as Mali (>300 $\mu g\ m^{-3}$) are much greater than the global average (21 $\mu g\ m^{-3}$).[139,57] However, little is known about the composition and diversity of airborne microbes in the Sahara region. The only prior study of airborne microbes in Mali used culture-based methods and open-face, collection with no size-selective inlet.[81] While it laid the foundation for future work, additional work using non-culture based detection methods is needed to fully capture the composition and diversity of these microbial communities.[69]

Most prior work on airborne microbes has focused on a single size fraction of dust, using one bulk sample collected on a filter or in an impingement medium.[81,47] Only a few studies have examined variability in the airborne microbial composition across particle size fractions,[10,95,19,123] and no size-fractionated data are presently available for the Sahara region. Such potential differences are important to understand because smaller atmospheric particles have greater propensity for long-range transport and also penetrate deeper into the lungs following inhalation, increasing risks to human health.[64,124]

Here, we investigate the influence of particle size on airborne bacterial abundance and diversity in Mali, West Africa during the Harmattan winds season under ambient (non-dust storm) conditions. We use these data to assess microbial transport propensity, which is inversely related to particle size. We use direct next-generation molecular sequencing of different sized dust samples obtained with-

out microbial culture to characterize microbial abundance (defined as 16S rRNA gene copy number per m^3) and diversity (defined as number of observed species and Faith's phylogenetic diversity) in the Sahara region. Our analysis provides better understanding of the composition, pathogenic potential, and transport propensity of microbes associated with atmospheric dust in a globally important source region.

1.1 Methods

1.1.1 Atmospheric Particle Sampling

We collected integrated daily atmospheric particle samples continuously between the hours of 9:00 and 19:00 over nine consecutive days between February 11-20, 2018 in Bamako, Mali. Sampling was intended to capture the time period of greatest human activity and exposure. Particle samples reflect both local and background sources. Samples were collected using a compact cascade impactor (CCI) that separated atmospheric particles into into five size fractions (>10.0, 10.0-2.5, 2.5-1.0, 1.0-0.5, and <0.5 μm), for a total of 45 individually analyzed samples. The CCI was designed and built by the Environmental Chemistry Laboratory at the Harvard T.H. Chan School of Public Health.[40]

No dust storms occurred on any of the sampling days. The duration of sampling averaged 7.7 hours per day, and the mean total volume of air sampled was 13.8 m^3 per day. All measures of microbial abundance were normalized by the volume of air collected because we were unable to obtain particle counts. The collection device was supported on a 1.52 m tripod, resulting in an inlet height 2 m above the Mali Météo building rooftop, which was 12 m above ground level (Table A.1). The collection site was located in a non-residential area 2 km away from Bamako International Airport to minimize the influence of commercial and residential vehicle traffic. The Météo building was the tallest structure within a 1-km radius without obstructions.

Inertial impactors with flat impaction substrates have been widely used as size-selective inlets,

collecting size-fractionated particles in ambient air.[98] These impactors remove larger particles, collecting the smaller particles on a downstream filter. However, when there are high particle concentrations, flat collection substrates allow some of the larger particles to bounce off due to their relatively high momentum and collect (along with the smaller particles) on the downstream filter. To overcome this limitation, an impactor was developed using porous polyurethane foam (PUF) as a substrate.[79] This substrate prevents bounce off and has higher loading capacity for the larger particles than flat substrates. Impactors with this substrate have been used successfully for sampling in desert regions during dust storm conditions.[22] This study used a cascade impactor with PUF for the largest four particle size fractions.[40] The last stage was a 47-mm diameter back-up filter. This last stage of the impactor has close to a 100% collection efficiency for particles with aerodynamic diameters <0.5 μm. Although the use of two different substrates (PUF and Teflon membrane filters) could introduce bias in percent recovery, we found no evidence for this in our data.

A constant flow rate of 30 L min^{-1} was maintained throughout sample collection. Field and laboratory blanks were collected and processed simultaneously with the samples. We chose not to sterilize the PUF substrates and filters to avoid damaging the substrates. None of the laboratory blanks contained amplifiable DNA, confirming the reliability of our approach. Face masks and gloves were worn during instrument calibration, setup, monitoring, dismantling, and sample handling to prevent contamination. All equipment was sanitized with sodium hypochlorite, ethanol, and UV irradiation between sample collection.[43]

At the end of each collection day, samples were processed in a laminar flow hood. PUF substrates and filters were individually submerged in a sterile solution of phosphate buffered saline and formalin in sterile storage tubes to satisfy international transport requirements. The phosphate buffered saline-formalin solution was made by buffering formaldehyde (37%) with sodium borate to a neutral pH and diluting with molecular-grade phosphate buffered saline to 2% final formaldehyde concentration. Storage tubes were immediately sealed with Parafilm tape and put into individual Whirl-Pak

(Whirl-Pak, Nasco, USA) bags. All samples and field blanks were stored at 4°C and transported by air to Harvard University (Cambridge, MA, USA). We compiled meteorological data from an Airmar WX200 weather station at the same time and location during sample collection (Airmar Technology Corp., Milford, NH, USA). Average meteorological conditions are summarized in the Appendix A Table A.1. We used the Hybrid Single-Particle Lagrangian Integrated Trajectory model (HYSPLIT[144], Version 4) to reconstruct 72-hour backward and forward trajectories and confirm the majority wind direction and origins of long-range air masses.

1.1.2 DNA Extraction, Sequencing, and Post-Processing of Reads

We used 16S ribosomal RNA gene amplicon sequencing to characterize the composition and diversity of airborne microbial communities across the five different particle size fractions. Genomic DNA was extracted from particle samples using the PowerSoil DNA Isolation kit (MoBio Laboratories Inc., Carlsbad, CA, USA) following the manufacturer's protocol, with modifications to account for the substrate materials. Each PUF substrate was cut into three pieces and extracted separately by adding it directly to the power bead mixture. Filter substrates were added directly to the power bead mixture. Substrate storage liquid was centrifuged and the pellet was added to the power bead mixture. The V4 hypervariable region of the 16S rRNA gene in both bacteria and archaea was amplified and sequenced in duplicate for each sample using the primer pair 515F (GTGYCAGCMGCCGCGGTAA)[119] and 806R (GGACTACNVGGGTWTCTAAT)[2]. These duplicates were employed as stochastic replications of the polymerase chain reaction (PCR) step to reduce potential bias. The 16S rRNA genes were amplified in a 30 cycle PCR using the HotStarTaq Plus Master Mix Kit (Qiagen, USA) under the following conditions: 94°C for 3 minutes, followed by 30 cycles of 94°C for 30 seconds, 53°C for 40 seconds and 72°C for 1 minute, after which a final elongation step at 72°C for 5 minutes was performed. After amplification, PCR products were checked in 2% agarose gel to determine the success of amplification and the relative intensity of

bands. PCR amplicons were then purified using calibrated Ampure XP beads (Beckman Coulter, USA) and pooled for sequencing. Sequencing was performed using an Illumina MiSeq platform (San Diego, CA, USA) following manufacturer's guidelines. DNA extraction and PCR amplification were performed on controls as well as negative lab controls using no template. DNA extraction kit and lab controls on the substrates did not amplify or sequence, indicating low risk for contamination. DNA extraction, amplification and sequencing of all samples were carried out at Molecular Research LP (Shallowater, TX, USA).

Sequence data were processed and analyzed using the Quantitative Insights Into Microbial Ecology (QIIME) pipeline, Version 1.9.[26] Quality filtering and processing of paired-end reads were performed following Mahmoudi et al.[97] The initial QIIME workflow involved pre-processing of the data by removing primers, demultiplexing, quality filtering to discard sequences with a quality score of <19 and removing chimeric sequences via USEARCH.[44] Sequences were then clustered into operational taxonomic units (OTUs) at 99% identity. Taxonomy was assigned based on the Greengenes (v13_8)[41] database using the ribosomal database project (RDP) classifier with an 80% confidence threshold.[102,166,162] Sequences present in <0.005% of the total data set were removed to limit the effect of spurious OTUs on analysis.[111] Analyses were performed after rarefying the samples to the same sequencing depth (27,680 sequences) using QIIME, R v.3.5.1[128], Phyloseq[103], and Vegan[115].

1.1.3 Determining Bacterial Abundance via Quantitative Polymerase Chain Reaction (qPCR)

Bacterial abundance was evaluated using qPCR amplification of the 16S rRNA gene using the bacteria-specific primer pair Bac2F (CCATGAAGTCGGAATCGCTAG) and Bac2R (GCTTGACGGGCGGTGT) in triplicate.[13] The qPCR mixture contained the following: 1 µM forward primer, 1 µM reverse primer, 500 nM Probe (BHQ; Integrated DNA Technologies, Inc., Coralville, IA), 1X Taq-

Man Universal PCR Master Mix (Applied Biosystems, Waltham, MA, USA) and 1.0 µL of template DNA. Bacterial 16S rRNA copy numbers were amplified and quantified with the StepOnePlus Real-Time PCR System (Applied Biosystems, Waltham, MA, USA). qPCR results were analyzed using StepOne Software Version 2.2.2.

1.1.4 Assessing the Presence of Potential Pathogens Using PCR

We identified the presence of species that are potential pathogens using PCR. Fifteen samples were tested for six different pathogens chosen based on qualitative evaluation of three properties: high absolute abundance in the samples at the genus level, detection in previous studies of airborne microbes, and degree of pathogenicity for humans. These included: *Bacillus cereus* (n=3 samples), *Escherichia coli* (n=3 samples), *Fusobacterium nucleatum* (n=4 samples), *Streptococcus pneumoniae* (n=1 sample), *Staphylococcus epidermidis* (n=4 samples), and *Pseudomonas aeruginosa* (n=1 sample) (Table A.2). Six different primer sets corresponding to the six species were used to perform PCR (Table A.3). For each of the six species tested, 2 µL of the template DNA was used to perform PCR using TaqMan Universal PCR Master Mix (Applied Biosystems) or PowerUp SYBR Green Master Mix (Applied Biosystems) in StepOnePlus Real-Time PCR System (Applied Biosystems). PCR was also performed using 1 µL of the PCR product after 10 cycles of the PCR reaction. PCR was carried out with an initial holding stage of 50°C for 2 minutes followed by 95°C for 10 minutes. The cycling stage consisted of 40 cycles of 95°C for 15 seconds, followed by 60°C for 1 minute. All PCR analyses were carried out at Molecular Research LP (Shallowater, TX, USA). Additional analyses are required to confirm the viability and strain of potential pathogens identified using PCR. This was not possible because samples had to be sterilized to satisfy international export requirements, precluding culture-based analyses and mRNA-based viability tests.

1.1.5 Statistical Analyses

Alpha diversity, or within-sample diversity, was evaluated using two metrics: Faith's phylogenetic diversity and number of observed species. Faith's phylogenetic diversity is a measure of diversity that accounts for the evolutionary relationships among OTUs in a community, and number of observed species represents the number of unique OTUs in a sample as a measure of species richness. Nonparametric analysis of variance on ranks (Kruskal-Wallis) followed by Dunn's multiple comparison test was used to evaluate statistical differences in: (1) microbial abundance (defined as 16S copy number per m^3), grouped by the sampling day or by particle size fraction; (2) alpha diversity, grouped by the sampling day or by particle size fraction; and (3) relative abundance of individual OTUs in different sample groups (by the sampling day and by particle size). Beta diversity, or between-sample diversity, was evaluated using the weighted UniFrac distance then visualized using principal coordinate analysis (PCoA) in R.[94]

1.2 Results and Discussion

1.2.1 Abundant and Diverse Microbes Are Present in All Size Fractions of Saharan Dust

Prior work has hypothesized that remote desert regions will have relatively low airborne microbial abundance compared to temperate and tropical regions.[25] By contrast, we found that bacterial abundance in the desert region of Mali sampled here (mean daily abundance 1.94×10^5 copies/m^3) was greater than previously reported for more urban regions and temperate latitudes. For example, summed abundance across all particle sizes in this study (Table 1.1) exceeds airborne microbial concentrations reported for Beijing, China in the summer (4.7×10^4 copies/m^3)[174] and during Asian dust events (average 9.4×10^4 copies/m^3).[172]

Table 1.1: Daily bacterial abundance* on different particle sizes out of the daily total.

	Particle Size (micrometers)						
Day†	<0.5	1.0-0.5	2.5-1.0	10.0-2.5	>10.0	Total	Air vol. (m^3)
1	4.34	6.11	7.77	10.2	30.4	58.8	10.6
	(1.32)	(0.491)	(1.80)	(4.21)	(6.40)		
percent	7	10	13	17	52	100	
2	3.98	20.5	25.6	203	279	532	13.0
	(0.836)	(20.8)	(13.3)	(42.8)	(11.9)		
percent	1	4	5	38	52	100	
3	3.74	7.57	23.4	40.2	97.8	172	9.24
	(0.876)	(1.27)	(2.88)	(14.0)	(12.4)		
percent	2	4	14	23	57	100	
4	4.45	9.35	13.8	20.1	63.0	111	15.0
	(0.840)	(1.53)	(1.03)	(5.79)	(4.02)		
percent	4	8	12	18	57	100	
5	2.54	7.44	7.89	10.7	46.1	74.7	13.3
	(0.702)	(0.834)	(2.02)	(3.98)	(22.2)		
percent	3	10	11	14	62	100	
7	17.1	19.9	12.5	83.4	154	287	16.4
	(22.7)	(22.0)	(2.42)	(21.0)	(42.6)		
percent	6	7	4	29	54	100	
8	6.45	6.61	6.06	21.3	51.7	92.1	15.3
	(1.68)	(0.469)	(0.863)	(7.95)	(29.1)		
percent	7	7	7	23	56	100	
9	2.01	3.17	8.35	16.4	31.2	61.1	15.1
	(0.158)	(1.57)	(2.91)	(7.09)	(4.25)		
percent	3	5	14	27	51	100	

*Abundance is shown as 10^{-3} 16S rRNA copies/m^3, with standard deviation in parentheses and percent abundance on each particle size shown as a percent of the daily total 16S rRNA copies/m^3.

†Day refers to consecutive sampling days in February 2018 in Bamako, Mali, West Africa.

To assess airborne bacterial diversity, our analysis of 16S rRNA gene amplicon sequences recovered a total of 3,111,322 high-quality sequences with an average read length of 252 base pairs. The sequences clustered into a total of 1,572 OTUs and 514 unique species. Rarefaction curves approached a saturation plateau (Figure A.1), and Good's coverage, an indicator of sampling completeness, ranged from 91% to 99%, indicating that the sequencing depth was sufficient to capture the diversity of each sample.[60] The one prior study from Mali, West Africa[81] identified a total of 94 bacterial isolates, which are sequences of bacteria identified using culturing.

1.2.2 Similar bacterial composition of near-field and far-field Saharan dust

Similarity in the composition of near-field and far-field Saharan dust suggests that some of the airborne community structure is retained during long-distance transport. For phyla, the top three most abundant ones observed in this study were Proteobacteria (34% mean relative abundance), Firmicutes (29%), and Actinobacteria (26%). These same three phyla were detected in the one previous culture-based study in Mali.[81] Saharan dust samples collected in Europe also contained Proteobacteria as the most abundant phylum.[104,136,6] Firmicutes have previously been associated with long-distance dust events that originated in the Sahara.[104,76,21] At the class level, Actinobacteria, Bacilli, and Gammaproteobacteria were the most abundant across all samples collected in this study (Figure 1.1b). Other important classes included Betaproteobacteria, Alphaproteobacteria, Clostridia, Bacteroidia, and Flavobacteria (Figure 1.1). Alphaproteobacteria, Actinobacteria, Betaproteobacteria, and Gammaproteobacteria were detected in Saharan dust intrusions in Spain (Figure 1.1).[59] Furthermore, Actinobacteria and Betaproteobacteria were abundant in samples of Saharan dust collected in the European Alps.[104]

At the family level, Betaproteobacteria families Oxalobacteraceae and Comamonadaceae were detected in this study and also abundant in Saharan dust collected in Spain.[70] Previous studies of air masses passing over the Sahara and collected in the Mediterranean indicate the presence of Gem-

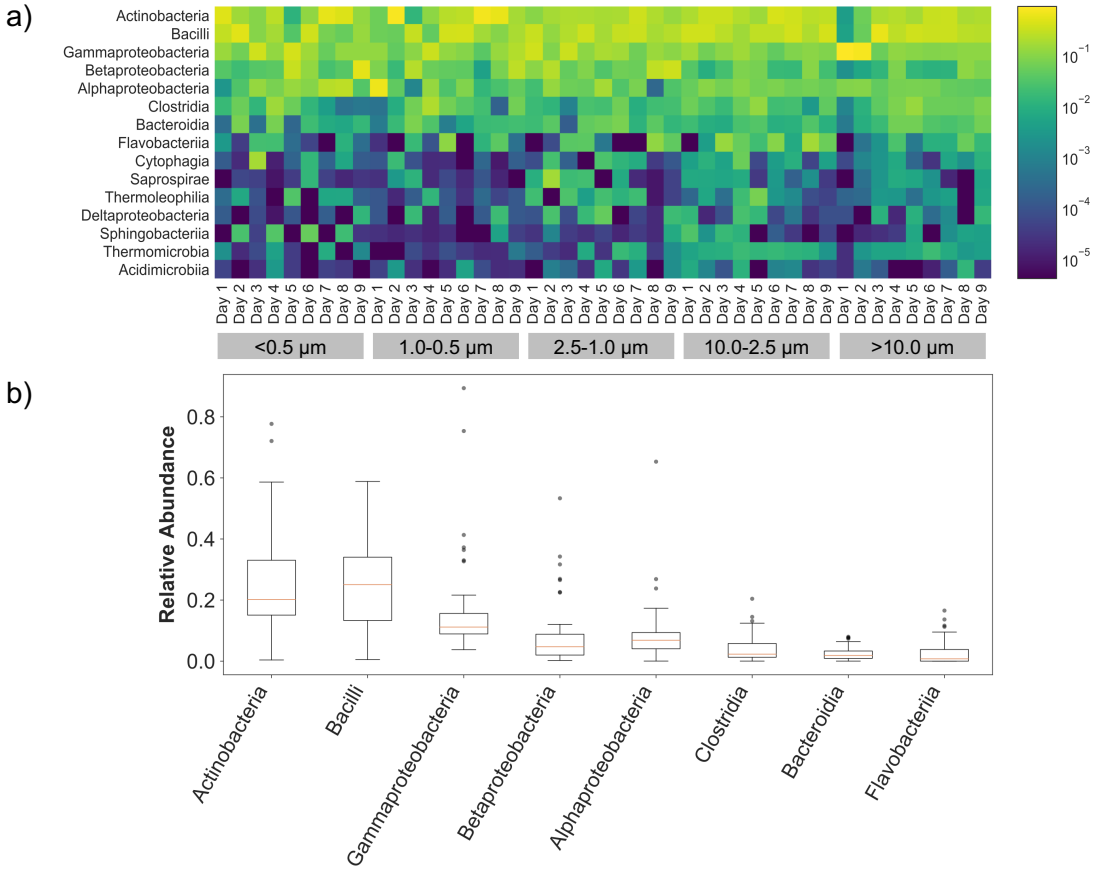

Figure 1.1: Dominant taxonomic composition of microbial community detected on atmospheric particles from Mali, West Africa. Panel a) shows relative abundance (log scale) of classes present in at least 80% of all dust samples. The x-axis shows individual samples grouped by particle size from smallest to largest fractions. Panel b) shows relative abundance of total OTUs represented by different microbial classes.

matomonadetes and Chloroflexi, which we also detected in this study.[78] Gemmatomonadetes are associated with soils from hyper-arid environments characterized by low biomass, including the Sahara Desert[49,36,31], and have been proposed as "bioindicators" for Saharan dust events.[104]

1.2.3 Similar patterns of variability in microbial abundance across most particle size classes

Total (summed) daily abundance varied by approximately an order of magnitude across the 9 sampling days from a minimum of 5.88×10^4 16S rRNA copies/m^3 on day 1 to a maximum of 5.32×10^5 16S rRNA copies/m^3 on day 2 (Table 1.1). The >10.0 μm size class contained the greatest fraction (51-62%) of total abundance across sampling days (Table 1.1). The smallest two size fractions of dust (<0.5 μm and 1.0-0.5 μm) each contained less than 11% of the total abundance.

We tested whether variability in microbial abundance followed the same daily patterns across particle size classes. Results showed that variability in daily abundance within each dust size fraction was well correlated with other particle size fractions, with the exception of the smallest size fraction (Figure 1.2, Spearman's $\rho > 0.71, p < 0.05$). The smallest size fraction (<0.5 μm) was not significantly correlated (Spearman's $\rho = -0.02 - 0.47, p > 0.05$) with all the other sizes. These results indicate that variability in microbial abundance across days is generally reflected by all size fractions of dust except those <0.5 μm. Most airborne particles less than 1 μm in diameter are formed in situ in the atmosphere rather than from surface resuspension because they are difficult to generate mechanically due to their large area to volume ratios.[74] Limited surface resuspension as a source of particles <1 μm could explain why microbial abundance is significantly lower for these particles compared to those >1 μm in diameter.

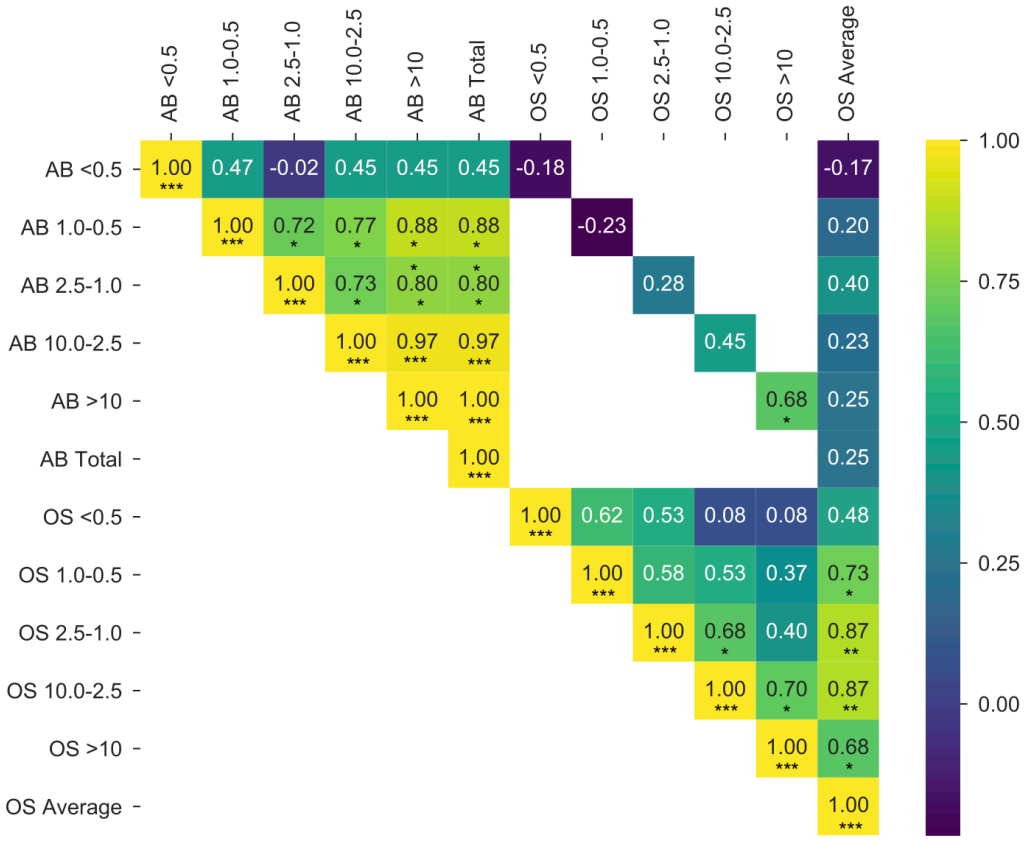

Figure 1.2: Spearman coefficient correlation matrix for abundance (AB, 16S rRNA copies/m^3) and observed species (OS, observed OTUs) across the different particle size fractions (>10.0, 10.0-2.5, 2.5-1.0, 1.0-0.5, <0.5 µm) on all days. Total abundance (AB Total) was calculated as the sum of the abundance across all particle sizes on each day. Average observed species (OS Average) was calculated as the average of all size fractions on each day. The color shows the strength of the positive association. Significant correlations are denoted by asterisks ($*p < 0.05; **p < 0.005; ***p < 0.0005$).

1.2.4 Abundance and Diversity Are Correlated for Larger Particles

We investigated whether large daily fluctuations in microbial abundance were correlated with variability in species diversity assessed by the number of unique OTUs detected on all particle size fractions. For particles of 0.5-10 μm diameter, abundance and diversity were not significantly correlated (Figure 1.2, Spearman's $\rho = -0.23 - 0.45, p > 0.05$). For >10 μm diameter particles, abundance and observed OTUs were significantly correlated (Spearman's $\rho = 0.68, p < 0.05$). Particles >10 μm have an extremely short lifetime against sedimentation.[74] Thus, they are likely derived from local sources compared to more diffuse sources for smaller particles. Such relatively large particles are not easily lofted by wind suggesting that they originate from local human activities such as agriculture.

When aggregated across all sampling days, we found statistically greater abundance (Figure 1.3, panel A) and diversity (Figure 1.3, panels B and C) in particles >2.5 μm compared to those <2.5 μm (Figure 1.3). Particles >10 μm had significantly greater abundance and diversity than the 2.5-10 μm size fraction (Figure 1.3). These results suggest that larger particles may contain species that differ substantially from the other particle sizes.

1.2.5 Unique Taxa Detected on Larger Particles

PCoA using the weighted UniFrac distance shows some clustering in taxonomic composition among larger particles but substantial scatter among the smaller size classes of particles (Figure 1.4a). These results are easier to visualize when samples are grouped by particles <2.5 μm and those >2.5 μm, with more clustering evident in the >2.5 μm size fractions (Figure 1.4b). This suggests that there may be some unique bacteria on larger particles that are not present on smaller ones, although two exceptions are present with substantially different taxonomic composition on days 1 and 2 (Figure A.2). Particles >2.5 μm likely cluster more together because they originate from similar local

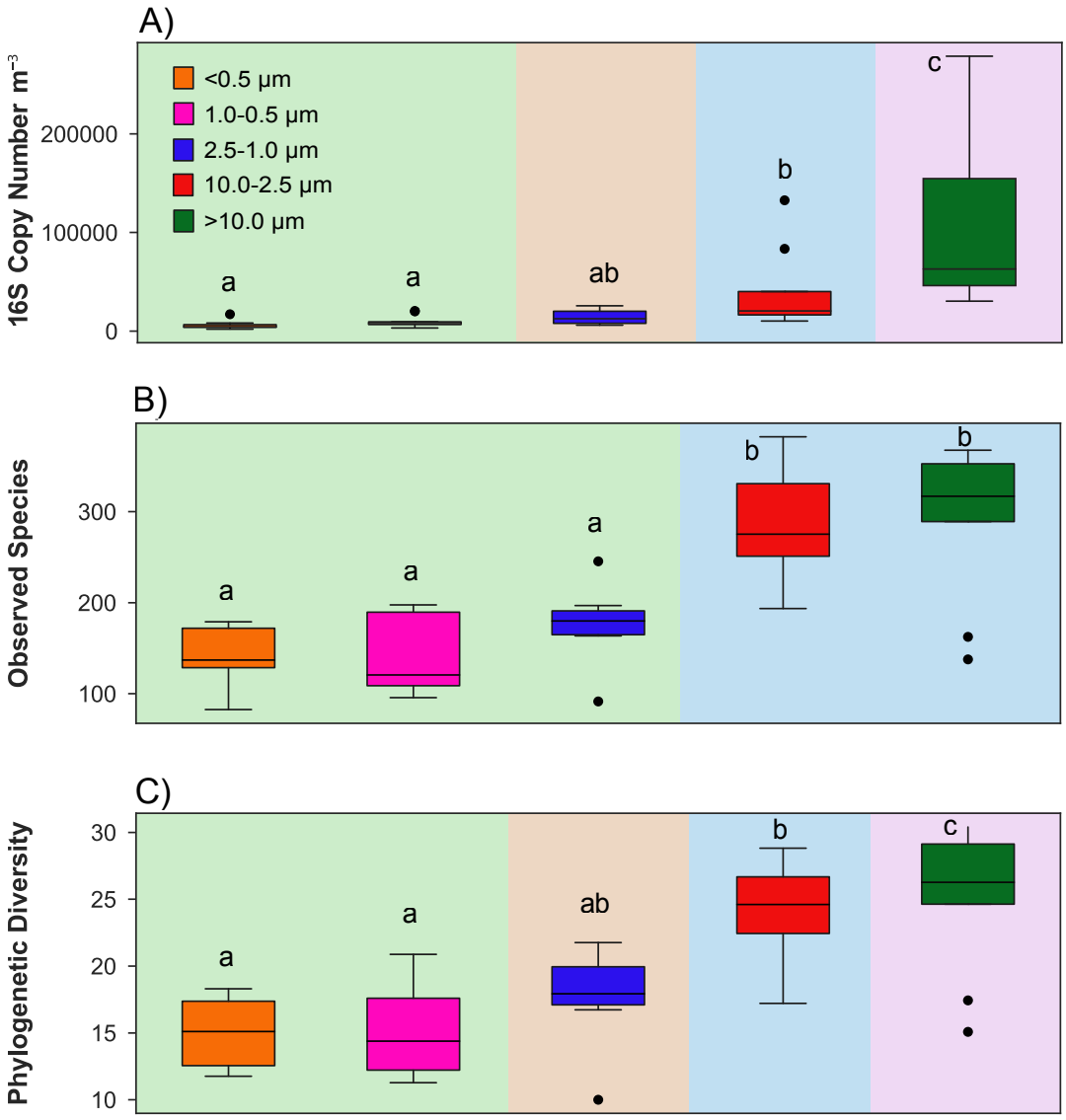

Figure 1.3: Effect of particle size on airborne microbial communities: (A) microbial abundance (16S rRNA copies/m^3 as estimated by qPCR) and averaged over each size fraction; alpha diversity as measured by (B) number of observed species and (C) Faith's phylogenetic diversity. Letters above boxes indicate similarities among groups (different letters indicate statistically significant difference, Dunn's test, $p < 0.05$; same letters = no difference).).

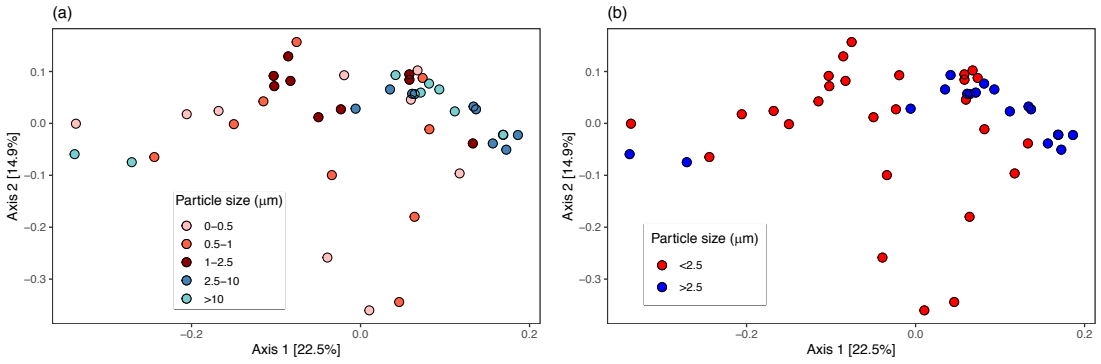

Figure 1.4: Community analysis using pairwise, weighted UniFrac distances visualized on a principal coordinates analysis (PCoA) plot with the percent of variation explained by each axis noted in brackets. Samples were grouped by (a) five particle size bins and (b) smaller (<2.5 μm) and larger (>2.5 μm) particle size bins. UniFrac is a metric for beta diversity (between-sample diversity) that measures the unique fraction of the phylogenetic distance between the taxa of two different samples.

sources, while smaller particles cluster less because they are more likely to be from a varied mixture of sources.[100]

Large particles contained the greatest number of OTUs and small particles contained the fewest (Figure 1.3). Because particles <2.5 μm contained significantly fewer species and had lower phylogenic diversity than those >2.5 μm, we hypothesized that some species would be preferentially found on specific size fractions of particles.

We found that 14 of the 1572 OTUs (0.9%) detected differed significantly in frequency across the five particle sizes and 170 differed between sizes <2.5 μm and those >2.5 μm (Kruskal-Wallis test, Benjamini-Hochberg (FDR) $p < 0.05$). Differences between these two size ranges are dominated by OTUs that appear in the larger size fraction but not the smaller size fraction. All 14 OTUs exhibited a preference for particles above 1 μm. Of the 170 OTUs, 162 were greater in the larger size fraction than the smaller size fraction. This implies that the day-to-day differences in OTUs across all sizes are dominated by changes in the larger size particle fraction originating from mainly local sources.

Bacterial cells are typically 1-2 μm in diameter or smaller.[38] Higher abundance and alpha diversity in larger particles (>2.5 μm), as well as the individual taxon preferences for the largest three

particle size fractions (Table A.4; Appendix A Additional Text), therefore implies that most microbial cells are either bound to soil particles or to each other as cell aggregates, rather than free-floating as individual cells.[161] However, abundant microbes on all particle size fractions means that we cannot preclude the existence of some freely suspended bacteria. Some of the OTUs that were in higher abundance in the larger size fraction than the smaller size fraction have been documented to aggregate, including *Pseudomonas*[154], *Geodermatophilus*[73,46], and *Corynebacterium*[117]. In the atmosphere, association with particles could improve survival of airborne microbes by providing nutrients as well as protection against UV exposure and desiccation (Table A.1).[90] Larger particles may provide more favorable conditions for survival or simply more crevice surface area that can harbor bacteria.

1.2.6 Presence of potential pathogens in Saharan dust

Atmospheric transport of viruses and fungi has been associated with disease outbreaks, such as foot-and-mouth disease and sea fan disease.[106,56] To date, no studies have linked long-distance airborne transport of bacterial pathogens with outbreaks of human disease. Out of the six species and 15 individual samples tested, seven samples contained four different potentially pathogenic species: *B. cereus*, *E. coli*, *P. aeruginosa*, and *F. nucleatum* (Table A.2). The presence of potential pathogens, particularly in smaller particle sizes, is of great interest because particles <2.5 μm penetrate deeply into the lungs and can enter the bloodstream once inhaled.[134] Future studies focused on assessing the viability and strain of these potential pathogens would be highly informative for understanding the extent to which long-distance airborne transport of pathogens poses a risk to human health. For example, certain strains of *B. cereus* are the causative agent of food poisoning, eye infections, pneumonia, sepsis, and central nervous system infections.[15] This potential opportunistic pathogen was present in two of the three samples tested, both of which were the smallest size fraction (<0.5 μm). *E. coli* was present in two of the three samples tested, in the smallest two particle size fractions (<0.5

μm and 1.0-0.5 μm). Pathogenic *E. coli* strains cause diarrhea and extraintestinal infections in humans.[33] Diarrhea is a significant problem in Africa and the third leading cause of death for children under five years old.[130] Previous research showed that proximity to cattle feedlots, dry cattle pen surfaces, and airborne dust are all positively correlated with a risk for airborne transport of *E. coli*.[9] *P. aeruginosa* was present in the only sample tested, which belonged to the 10.0-2.5 μm size fraction. This potential opportunistic pathogen is most commonly associated with respiratory infections, and some pathogenic strains are particularly problematic given their potential for antibiotic resistance and ability to survive in different environments.[135] *P. aeruginosa* has been isolated from foods such as the West African Mud Creeper sold in local markets.[1]

The one prior study of airborne microbes in Mali found that up to 25% of the bacterial isolates detected were opportunistic human pathogens.[81] Many of the genera phylogenetically related to human pathogens, as well as two of the potential pathogens confirmed at the species level using PCR, exhibited abundance in the smallest particle size fractions (<2.5 μm), highlighting the potential for long-distance transport. The 72-hour forward trajectories for all sampling days extended from the Northeast beyond the continent and into the Atlantic Ocean, illustrating the path of this long-distance transport (Figure A.3c, Figure A.4).

1.3 Implications

Results of this work show abundant and diverse microbes in all five size fractions of dust from a desert region of Mali, West Africa. Prior studies have hypothesized that microbial abundance and diversity will be relatively low in arid desert regions[25,52] but our results show they are similar to temperate regions. Since bacterial cells are typically 1-2 μm in diameter or smaller,[38] presence of more detectable bacteria on larger particle size fractions suggests most are aggregated on particles or other cells. The microbial community detected in Mali contained similarities at the phylum, class,

and family level to prior studies conducted in destination regions from the Sahara, suggesting some of the microbial community structure is retained following long-distance transport.

We observed substantial daily variability in microbial abundance, with similar patterns across most particle size fractions. One exception was low abundance that did not follow other size fractions for <0.5 μm diameter particles. These ultrafine particles are generated primarily in the atmosphere and are difficult to suspend from local sources, suggesting a different origin than other particle size fractions.[74] Daily variability in abundance was not correlated with diversity for most of the particle size fractions, with the exception of >10 μm diameter particles. Such large particles are difficult to suspend by wind only and have a short atmospheric lifetime, therefore likely reflect local human activity.[74]

Larger particles, with more localized origins, contained the greatest proportion of species diversity. Of the 1572 OTUs detected in this study, 162 were preferentially present on particles >2.5 μm in diameter. This implies some bacteria are preferentially aggregated on large particles. Greater abundance on larger particles may reflect more favorable conditions or greater crevice area allowing better survival. Overall, our results suggest the composition and sources of airborne microbes can be better discriminated by sampling programs that collect size-fractionated samples. A limitation of this study was lack of access to a particle counter in this remote field setting and particle concentrations were instead normalized to volumes of air sampled. Future studies of microbial composition would benefit from size fractionated microbial samples collected simultaneously with aerosol concentrations.

Potential human pathogens were found using PCR in all size fractions of dust tested, including the smaller particles that are more likely to undergo long distance transport. A limitation of our work was that we were unable to test the strain and viability of these pathogens using typical culture-based assays because international transport restrictions required that dust samples be sterilized. Such bacteria are therefore excellent candidates for viability and strain testing in future studies

of dust from Saharan source regions.

There are bred certain minute creatures that cannot be seen by the eyes, which float in the air and enter the body through the mouth and nose and there cause serious diseases.

Marcus Terentius Varro, 36 BC

2

Characterization of Hospital Airborne SARS-CoV-2

Reproduced with permission from: Stern, R.A., Koutrakis, P., Martins, M.A., Lemos, B., Dowd, S.E., Sunderland, E.M. and Garshick, E., 2021. Characterization of hospital airborne SARS-CoV-2. *Respiratory Research*, 22(1), pp.1-8.

The rapid spread of coronavirus disease 2019 (COVID-19) raises questions about guidelines regarding droplet and aerosol exposure control measures. Recent studies emphasize the potential for airborne transmission. [120,67,108,107,160,54] However, there is ongoing debate about the potential for aerosol transmission of the disease and the particle size responsible for it. Larger particles are generated by coughing [173] and sneezing [17], while smaller particles are emitted during speaking and formed by secondary processes such as particle aging or evaporation. [3] Smaller particles remain airborne for longer periods of time and may travel farther than the six-foot (1.83 m) separation distance recommended during the current pandemic. [5] Fine particles ≤2.5 μm penetrate deeply into the lungs, particles 10.0-2.5 μm mainly deposit in the larger tracheal-bronchial airways, and particles >10.0 μm deposit in the upper respiratory tract. The size of the particle impacts the likelihood of infection by inhaled pathogens. [150]

Severe acute respiratory syndrome coronavirus 2 (SARS-CoV-2) [34], the virus that causes COVID-19, has been found to be viable in the air. [84] However, there have been limited efforts to identify the size fraction of particulate matter (PM) associated with airborne SARS-CoV-2. In hospital patient areas and a medical staff office in Wuhan, China, three samples were collected into distinct size fractions (>2.5 μm, 2.5-1.0 μm, 1.0-0.5 μm, 0.50-0.25 μm, and <0.25 μm). [92] The authors found SARS-CoV-2 RNA was associated with smaller size fractions near protective apparel removal rooms and with larger sizes in the medical staff office. In Singapore, three size-fractionated samples were collected in a patient's room with SARS-CoV-2 RNA detected in 1 to 4 μm and >4 μm size fractions. [29] These findings suggest that SARS-CoV-2 RNA may be found in aerosols in hospital areas near and where COVID-19 patients receive care.

Determining the size of particles carrying viral RNA is critical to understanding their respiratory tract deposition, health impact, residence time in ambient air, and potential for longer distance transport. Other than one study conducted inside the Nebraska Biocontainment/National Quarantine Unit [138], air monitoring has not been conducted in a U.S. hospital caring for COVID-19

patients. Little is known about the presence of the virus in hospital areas that are not directly involved in known COVID-19 patient care. There is no experimental data regarding the effectiveness of airborne control measures instituted by hospitals in response to the pandemic.

Boston was one of the first U.S. cities to be severely impacted by COVID-19 in 2020. This study was conducted at the Veteran's Affairs (VA) Boston Healthcare System in West Roxbury, Massachusetts, USA, a medium-sized hospital (134 staffed beds during the study) and the major VA medical center in the Boston area. To deal with the large influx of COVID-19 patients, existing wards were converted entirely to negative pressure ventilation areas requiring full personal protective equipment (PPE) to enter. Hospital locations nearby and outside these isolation units were heavily trafficked by staff. It is important to investigate whether these isolation procedures were effective in eliminating airborne SARS-CoV-2 RNA in neighboring hospital areas. In this study, for the first time, we simultaneously collected airborne particles of three size ranges, >10.0 μm, 10.0-2.5 μm, and ≤2.5 μm, in an acute care hospital environment in locations outside of COVID-19 patient care areas and in non-COVID wards to examine the size of particles and locations associated with SARS-CoV-2 RNA.

2.1 Methods

2.1.1 Collection Design

We used a micro-environmental cascade impactor designed and custom-built by the Environmental Chemistry Laboratory at the Harvard T.H. Chan School of Public Health (Figure 2.1).[39] This sampler simultaneously collects airborne particles in three size ranges. Large particles (>10.0 μm) and coarse particles (10.0-2.5 μm) are collected on polyurethane foam (PUF) impaction substrates. Fine particles (≤2.5 μm) are collected on a 37-mm glass fiber filter (GFF). The box contains a pump (VP0125, Medo, USA) that provides a constant flow rate of 5 liters per minute. Appendix B section

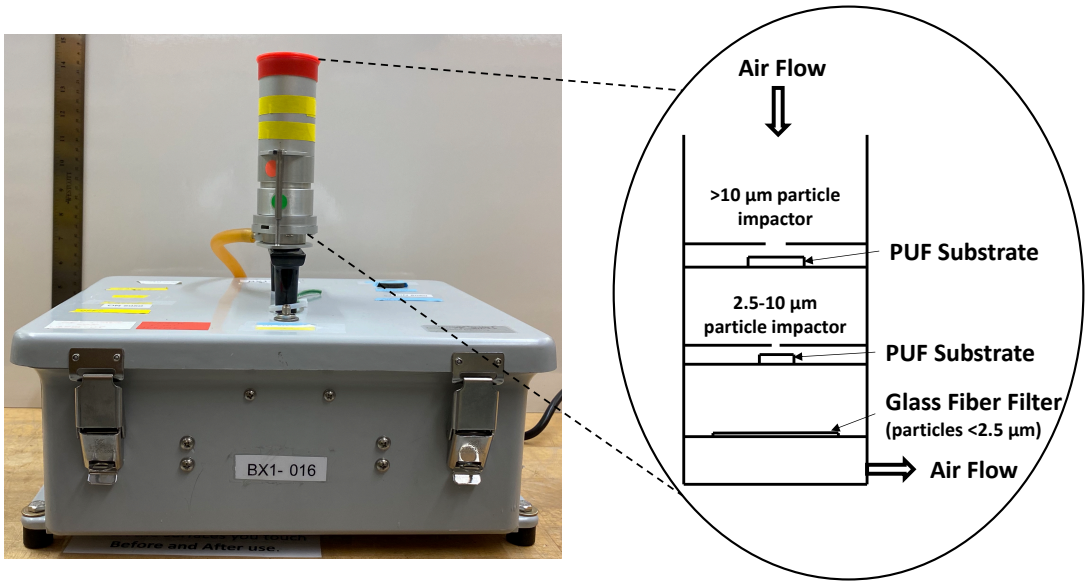

Figure 2.1: Micro-environmental cascade impactor designed and custom-built by the Environmental Chemistry Laboratory at the Harvard T.H. Chan School of Public Health (HSPH). PUF = polyurethane foam.

"Sample collection details" includes additional protocol information.

2.1.2 Setting and Sampling Scheme

Five sites were sampled simultaneously (Table 2.1) six times from April 29 through May 22, 2020. Each sample ran for 48 hours at a constant flow rate of 5 L/min for a total volume of 14.4 m^3 per sampling period. Samplers were located: (1) outside the entrance to a COVID-19 ward (CW1); (2) in a personal protective equipment (PPE) donning room outside the entrance to another COVID-19 ward (CW2); (3) outside the entrance to the medical intensive care unit (ICU); (4) at a staff workstation in the emergency department (ED); and (5) at a nursing staff workstation of a ward not designated for care of COVID-19 patients (NCW) (Table 2.1). CW1 was closed for cleaning from May 12-18, 2020 but sampling continued throughout this period. Additional details of the sampling locations are provided in Appendix B section "Sampling location details." Anyone en-

tering the ICU, CW1, and donning PPE in CW2 passed in proximity to the sampler because these three locations were at the entry points to the patient care units. Hospital policy during the sampling period included universal masking for staff and patients when outside their rooms, restricted visitation, and universal admission testing during the time period of the study.

The cascade inlets were located approximately at breathing zone height, 48 to 56 inches above the floor. Field blanks were used and processed simultaneously with the samples. Blanks were taken to the hospital together with the samples but were not exposed to air flow.

Table 2.1: Sampling locations. ED = Emergency Department; ICU = intensive care unit; CW1 = COVID-19 Ward 1; CW2 = COVID-19 Ward 2; NCW = Non-COVID-19 Ward.

Location Code	Brief Description	Details
ED	Emergency department provider workstation	Provider computer workstation across from two-negative pressure rooms used for suspect COVID-19 patients
ICU	Outside entrance door to COVID-19 ICU	In a corridor outside main entrance to the COVID-19 medical ICU
CW1	Corridor outside COVID-19 ward entrance	Midway through the study (May 12-18, 2020), this location was closed and cleaned; vacant on May 19; and later opened May 20 as a non-COVID-19 ward that includes a smaller unit that cared for suspected COVID-19 patients.
CW2	PPE donning room outside COVID-19 ward	PPE donning room that exits into a corridor to a second COVID-19 medical ward
NCW	Nursing workstation in non-COVID-19 ward	Open work area with computer workstation to chart patient notes and exchange information at shift changes

2.1.3 Processing

After each collection, the substrates were removed aseptically from the cascades, placed individually inside 5-mL sterile centrifuge tubes, immersed in RNAlater Stabilization Solution (Ambion, Inc., Austin, TX, USA), and stored in sterile Whirl-Pak (Whirl-Pak, Nasco, USA) bags at 4°C.

2.1.4 Sample Analysis

Samples and blanks were shipped overnight on ice to Molecular Research DNA (Shallowater, TX, USA), where RNA extraction and reverse transcription quantitative polymerase chain reaction (RT-qPCR) were performed. Viral RNA was extracted using the RNeasy Mini Kit (Qiagen, Hilden, Germany) following the manufacturer's instructions. 5.6 µg Poly-A carrier RNA (Qiagen, Hilden, Germany) was also mixed with each sample for extraction. Carrier RNA enhances the low copy viral nucleic acids binding to the mini column and also reduces the chance of viral RNA degradation. RNA was eluted in 40 µL RNase free water. RNA quantity and quality were determined using NanoDrop2000 (Thermo Scientific, Waltham, MA, USA). Samples were then used to quantify the viral concentrations by qPCR using 2019-nCoV CDC qPCR probe assays (Integrated DNA Technologies, Inc., Coralville, IA, USA) for the nucleocapsid N gene (Table B.1). 12 µL of RNA sample was used for cDNA synthesis using QuantiTect Reverse Transcription kit (Qiagen, Hilden, Germany). 2 µL of the synthesized cDNA was used to perform qPCR using 2X PrimeTime Gene Expression Master Mix (Integrated DNA Technologies, Inc., Coralville, IA, USA) in the StepOnePlus Real-Time PCR System (Applied Biosystems, Waltham, MA, USA). The qPCR reaction was carried out with an initial holding stage of 95˚C for 3 minutes for PCR enzyme activation. The cycling stage consisted of 45 cycles of 95˚C for 5 seconds, followed by 55˚C for 30 seconds. Genomic RNA from SARS-CoV-2 (2019-nCoV/USA-WA1/2020; ATCC, Manassas, VA, USA) was used as a standard. Positive samples were identified as those with a cycle threshold cutoff of 40.85 that

corresponded to one copy number. One sample was selected at random for shotgun sequencing to further evaluate SARS-CoV-2 RNA. The section "Shotgun Sequencing" in Appendix B describes complete methods and clade assignments. Genome sequences were submitted to GenBank [32] (accession number MW047086) and analyzed using NextStrain. [66]

2.1.5 Data Analysis

The method for calculating air concentration (copy number per m^3) is provided in Figure B.1. The probability of a positive sample for each sampling period was calculated as the number of positive size-fractionated samples divided by 15 (the number of size-fractionated samples collected per sampling period). Pearson correlation analysis was used to assess the association between the number of hospitalized COVID-19 patients and the probability of detecting a positive sample and new cases in Massachusetts19 (averaged over the sampling dates).Associations were also assessed between the probability of a positive sample in the ED and number of ED patients, including those with respiratory complaints.

2.2 Results

2.2.1 Air Concentrations of SARS-CoV-2

Table 2.2 presents the air concentrations (copies m^{-3}) of SARS-CoV-2 RNA in five areas of the hospital over six sampling periods per location. Concentrations ranged from 5 to 51 copies m^{-3}, with an overall rate of positive samples of 9% of the 90 size-fractionated samples. All field and laboratory blanks were negative for SARS-CoV-2 RNA by PCR. The highest concentrations were observed in the emergency department (ED) on May 13-15 at 51 copies m^{-3} (Table 2.2). The second highest concentration occurred at the non-COVID-19 ward nurse's station (NCW) on May 11-13 at 47 copies m^{-3}.

Table 2.2: Concentration of SARS-CoV-2 (copies m^{-3}) for each 48-hour sampling period starting the morning of the start date. ED = Emergency Department; ICU = intensive care unit; CW1 = COVID-19 Ward 1; CW2 = COVID-19 Ward 2; NCW = Non-COVID-19 Ward. F = fine, ≤2.5µm; C = coarse, 2.5-10 µm; L = large, ≥10 µm.

Dates (start - end)	Size	ED	ICU	CW1	CW2	NCW	Probability of positive sample	Average number of COVID-19 patients in hospital
20 April-1 May	F C L	0 0 0	7 0 5	0 0 0	0 0 0	0 0 12	3/15	33
5 May-7 May	F C L	0 8 0	0 0 0	0 0 0	0 0 0	0 5 0	2/15	24
11 May-13 May	F C L	0 0 0	0 0 0	0 9 0	0 0 0	0 0 47	2/15	17
13 May-15 May	F C L	51 0 0	0 0 0	0 0 0	0 0 0	0 0 0	1/15	14
18 May-20 May	F C L	0 0 0	0 0 0	0 0 0	0 0 0	0 0 0	0/15	9
20 May-22 May	F C L	0 0 0	0 0 0	0 0 0	0 0 0	0 0 0	0/15	7
Number of positive samples		2	2	1	0	3		
Total number of samples (size fractions)		18	18	18	18	18		

Designation as a COVID-19 ward was not associated with a greater prevalence of positive samples. The location with the highest prevalence of positive samples was the NCW (17%) (Table 2.3). The locations with COVID-19 patients – COVID-19 Ward 1 (CW1), COVID-19 Ward 2 (CW2), and intensive care unit (ICU) – had the lowest prevalence of positive samples (6% combined). CW1 had only one positive sample, and it did not occur when the ward was used for patient care, but rather when the ward was closed and being cleaned. CW2 was the only location without any positive samples. The ED staff workstation had a prevalence of positive samples equal to 11%.

Table 2.3: Number of positive samples detected in each location by size fraction. ED = Emergency Department; ICU = intensive care unit; CW1 = COVID-19 Ward 1; CW2 = COVID-19 Ward 2; NCW = Non-COVID-19 Ward.

	Fine (≤2.5 μm)	Coarse (10.0-2.5 μm)	Large (>10.0 μm)	Total
ED	1	1	0	2
ICU	1	0	1	2
CW1	0	1	0	1
CW2	0	0	0	0
NCW	0	1	2	3
Total	2	3	3	8

2.2.2 Particle Size Association

Viral RNA was detected in all size fractions with about the same frequency (Table 2.3). The ED had positive samples in the fine (≤2.5 μm) and coarse (10.0-2.5 μm) particle size fractions. Outside the ICU, SARS-CoV-2 RNA was detected in the fine and large (>10.0 μm) size fractions. Positive samples from the NCW were found in the coarse and large size fractions. The greatest concentration (51 copies m^{-3}) occurred in the fine size fraction in the ED. The second greatest concentration (47 copies m^{-3}) occurred in the large size fraction in the NCW.

2.2.3 Association With COVID-19 Patients

There was a significant positive association between the probability of detecting a positive sample and the average number of COVID-19 patients in the hospital during each sampling period ($r = 0.95, p < 0.01$). The number of COVID-19 cases in the hospital was positively associated with the number of new COVID-19 cases in Massachusetts averaged over the corresponding sampling period ($r = 0.99, p < 0.01$). The two greatest concentrations occurred on May 11-13 and May 13-15 when COVID-19 patient density in the hospital was not at its highest (Table 2.2). There was no association between the probability of a positive sample in the ED and the number of patients in the ED or the number of patients evaluated with respiratory complaints in the ED (Table B.2). The only positive samples outside the ICU occurred during the sampling period from April 29-May 1, when the hospital COVID-19 burden was at its highest (Table 2.2).

2.3 Discussion

Although SARS-CoV-2 RNA was present in 9% of all samples, no positive samples were found in the vicinity of CW1 or CW2 while they were used for patient care. The only positive sample in CW1 occurred while it was closed for cleaning. During this time, the negative pressure exhaust system was no longer in use, the ward doors were open, and cleaning crews were passing by the sampler to sanitize the ward. Other studies have documented positive air samples collected in COVID-19 patient rooms.[92,29,138] Our finding of no viral RNA outside of the COVID-19 wards while they were active (and only one positive sample outside the ICU) suggests that the negative pressure units were effective in limiting airborne exposure outside the units. Previous studies have shown that inside COVID-19 wards, including inside patient rooms, airborne SARS-CoV-2 RNA is detectable.[92,29,138]

Unexpectedly, the nurse's station on the non-COVID 19 ward (NCW) had the greatest number

of positive samples. We observed frequent congregation of staff and consultants at this location. Although it was policy for all hospital personnel to wear masks, it is possible that the positive samples were due to breaches of mask-wearing. The lack of association between the number of patients in the ED and the probability of a positive sample in the ED may be due to the fact that the patients in the ED were not predominantly COVID-19 patients, and the positive samples may instead reflect staff activity and patient flow near the ED workstation. The finding of greater positive rates in non-COVID-19 locations, in conjunction with the positive association between probability of a positive sample across all locations and the number of COVID-19 patients in the hospital, suggests that presence of SARS-CoV-2 RNA in the hospital reflects the disease burden more broadly in the community. This conclusion is supported by the strong positive association between the number of COVID-19 patients in the hospital and average daily new cases in Massachusetts.

The fact that we found concentrations in all particle size fractions suggests that virus-containing particles are from sources at different proximities to the sampler or produced by different mechanisms. SARS-CoV-2 RNA on larger particles, such as those in the NCW, may have been due to a cough by someone located near the sampler. Coughing generates larger particles than speaking.20 Viral RNA that was associated with smaller particles, such as that found in the ED, may reflect a greater distance between the sampler and source, formation of smaller aerosols from larger droplets (e.g., by evaporation), or production by processes emitting smaller particles (e.g., speaking as opposed to coughing). Finding positive samples during the cleaning period in CW1 may be due to resuspension caused by cleaning. We found these particles in the coarse (10.0-2.5 μm) size fraction. Liu et al. (2020) suggested that lofting of coarse particles may be caused by resuspension of particles from floors and hard surfaces. [92]

This is the first study to document the presence of SARS-CoV-2 RNA in size-fractionated air samples in non-COVID-19 areas in a U.S. hospital. Previous efforts to study COVID-19 have been focused in COVID-19 patient care areas, with samplers located close to the source (infected

patients) and collected onto a single bulk filter to analyze total suspended particulate (TSP). Santarpia et al. (2020)[138], Ong et al. (2020)[116], and Ding et al. (2020)[42] all collected only TSP. Liu et al. (2020) collected samples in Wuhan, China that were mostly TSP, with only three size-segregated samples.[92] Chia et al. (2020) also collected only three size-segregated samples.[29] We detected maximum concentrations on the same order of magnitude as the size segregated samples of Liu et al. (51 copies m^{-3} in our study; 42 copies m^{-3} for Liu et al., 2020).[92] Liu et al. (2020) found higher concentrations of SARS-CoV-2 RNA in the fine PM fraction than in larger sizes.[92] Chia et al. (2020) had positive samples in the 4-1 μm size fractions.[29] These results support our finding of SARS-CoV-2 RNA associated with fine particles that are capable of long-distance transport.

We detected a greater percentage of positive samples compared to some previous studies. The percent of positive samples was greater in our study (9%) than in the study by Ong et al. (2020) (0%) and Ding et al. (2020) (2%), despite the fact that these studies were conducted in COVID-19 patient care areas.[116,42] Potential explanations for our higher positive sample rate may be related to a greater viral load in the air or methodological differences. For instance, our study collected a greater volume of air per sample (14.4 m^3) compared to these studies (1.2 and 1.0 m^3, respectively) and more samples.

The percentage of positive samples was smaller in our study compared to Chia et al. (2020) (67%), Liu et al. (2020) (77%), and Santarpia et al. (2020) (58-63%).[92,29,138] A possible explanation is the proximity to the source: Chia et al. collected only in airborne infection isolation rooms of COVID-19 patients[29], and Santarpia et al. collected only inside the Nebraska Biocontainment/National Quarantine Unit.[138] Liu et al. sampled under conditions of higher disease prevalence (in Wuhan in February and March 2020).[92] Differences in extraction efficiency from the collection substrate, variability in RNA degradation rates, or differences in PCR sensitivity among studies may also explain the differences in rates of positives samples and air concentrations.

The estimation of airborne virus concentrations (copies m^{-3}) assumes that there is a continuous

emission source. However, it is more likely that the emissions of the virus occurred as isolated events (e.g., a sneeze, cough, or speaking) from infected people rather than as a continuous flux over the entire 48-hour sampling period. Since the calculated concentrations are time-weighted averages, someone exposed at the time of emission would likely receive a larger dose over a shorter time period than those implied based on the calculated concentrations.

While the present study detected SARS-CoV-2 RNA in hospital air samples, it did not determine whether the airborne virus was viable (capable of causing infection). Lednicky et al. (2020) recently reported that SARS-CoV-2 in hospital air is infectious.[84] Santarpia et al. (2020) found viable SARS-CoV-2 in particles <1 μm.[137] Laboratory-generated aerosols containing SARS-CoV-2 were found to remain infectious for three[157] to 16 hours.[50] The infectious dose of SARS-CoV-2 is still unknown. It is possible that the infectious dose of SARS-CoV-2 is similar to that of SARS-CoV-1,[7] which was estimated to require 280 viral particles to cause illness in 50% of people.[163] The concentrations measured in the present study are likely underestimated, which may be attributable to losses during extraction from the substrates, RNA degradation, and the sensitivity of PCR, as we detected SARS-CoV-2 RNA by shotgun sequencing in a sample near the lower limit of PCR detection (See Appendix B section "Shotgun Sequencing").

2.4 Conclusion

The COVID-19 pandemic has challenged preconceptions about virus transmission. Our findings support changes in guidance from international bodies including the World Health Organization that help prevent airborne transmission of the virus. The findings promote universal masking for patients and providers and social distancing, even in non-COVID-19 hospital areas, to prevent future spread during this pandemic. Hospital policies such as construction of negative pressure controls in existing wards appear to be effective in reducing airborne concentrations of the virus. The

fact that positive samples were concentrated in regions of the hospital with greater congregation of personnel indicates that airborne viral RNA exposure most likely occurs where the concentration of humans is greatest, regardless of whether or not those areas are dedicated for COVID-19 patient care. It suggests that greatest risk of airborne transmission occurs in areas that are treated socially or anecdotally as less risky with respect to COVID-19 exposure. Presence of the virus with fine particles highlights the potential for virus-laden particles to remain airborne for several hours and to penetrate deeply into the lungs. The implications of this research are not limited to hospital settings. Awareness of the aerosol transport of SARS-CoV-2 with fine PM may help to reduce transmission and support rationale for discouraging potential super-spreader events.[87]

Messieurs, c'est les microbes qui auront le dernier mot.

Luis Pasteur

3

Levels and Particle Size Distribution of Airborne SARS-CoV-2 at a Healthcare Facility in Kuwait

Coronavirus Disease 2019, (COVID-19) spread rapidly around the world and challenged existing conceptions of disease transmission and prevention.[16] Severe acute respiratory syndrome coronavirus 2 (SARS-CoV-2), the virus that causes COVID-19, was recently shown to remain viable in aerosols for up to 16 h.[157,142,50] However, little is known about the size distribution of SARS-CoV-2 in indoor and outdoor air. This property of airborne SARS-CoV-2 is essential for predicting the spread of the disease.

Of particular concern, healthcare workers are at increased risk of occupational exposure to SARS-CoV-2. The U.S. Occupational Safety and Health Administration (OSHA) now recommends airborne precautions to protect healthcare workers with exposure to the virus.[156] While many hospitals around the world grapple with risk reduction strategies for frontline healthcare workers during the pandemic, there is also notable nosocomial COVID-19 transmission among inpatients.[132] Infection control strategies aim to curb such risks as well as improve the resilience of healthcare workers. It becomes imperative to understand the role of air particles that serve as vectors for SARS-CoV-2 in the hospital workplace in which conventional infection control strategies may fall short.

Traditionally, the medical community has relied on the dichotomy of droplet (large particles that behave like projectiles) and aerosol (smaller particles that remain airborne for longer periods and can be inhaled) to characterize host-to-host transmission mechanisms. This is essential for risk management and allocation of resources to control respiratory infectious diseases.[169] In the COVID-19 pandemic, authorities stressed the importance of droplet transmission. However, breathing, talking, singing, and coughing release particles of a continuum of sizes.[77] Even larger particles that are produced from processes such as coughing[173] and sneezing[17] may dry out and become smaller.[165] Evidence suggests that smaller aerosols, including those generated by speaking, may be a vector for COVID-19.[108,107,114,143] These smaller particles have significant health impacts, as they are capable of penetrating deeper into the lungs. In other respiratory diseases, pathogens on smaller particles require fewer microorganisms to cause an infection than those on larger particles.[150,112,148]

A wealth of air pollution studies have shown that fine particulate matter (≤2.5 μm) remains airborne for several hours before being removed from the air by gravitational settling.[165,71,91,171,5] As a result, smaller particles can travel farther than 1 m, which is the social distancing space currently recommended by the World Health Organization,[170] and have a greater opportunity to infect someone who crosses their path. Information about the size distribution of airborne particles carrying SARS-CoV-2 is useful to model expected transmission distance and establish maximum coverage by airborne precautions.

Despite the important implications of the SARS-CoV-2 size distribution, there is little information about its presence with airborne size-specific particles in indoor and outdoor locations. Recent studies are extremely limited in scope. Early in the pandemic, Liu et al. (2020)[92] and Chia et al. (2020)[29] collected three times each in healthcare settings. Lednicky et al. (2021)[85] examined aerosols inside a car driven by a patient with COVID-19, with one collection in five individual size fractions. Santarpia et al. (2020)[137] collected aerosols inside the rooms of COVID-19 patients six times, for a total of 18 individual size-fractionated samples. Stern et al. (2021)[146] collected 30 times in three size fractions inside a U.S. hospital. There are still unanswered questions about the severity of risk of small particle-associated COVID-19 transmission and the likelihood of location-dependent viral RNA concentrations in the air.

In this over two-month-long study, we present the most comprehensive COVID-19 air-sampling program in healthcare workplaces to date, with 70 collections and 210 individually analyzed size-fractionated samples. We collected simultaneous air samples in three different size fractions at over 30 hospital locations including intensive care units (ICUs), nurses' workstations, the rooms of inpatients with and without symptoms, observation rooms (transitional treatment units in the Emergency Department where patients are continuously evaluated before the decision to admit or discharge), locker rooms, bathrooms, a lobby, waiting areas, patient hallways, swab testing areas, and outside hospital entrances. We examined the size distribution of SARS-CoV-2 in airborne particles

in three distinct size fractions: fine particles ≤2.5 μm (which are small enough to remain suspended in the air and penetrate deep into the airways and directly into the bloodstream), coarse particles 2.5-10 μm (which are inhalable but do not penetrate deeply into the lungs), and large particles ≥10 μm (which have relatively high settling velocities and travel shorter distances before settling out of the air). We hypothesized that SARS-CoV-2 RNA would be present in indoor air in different size fractions, including fine particulate matter, and that the aerodynamic size distribution would depend on the sampling location.

3.1 Methods

3.1.1 Site

Jaber Hospital is located in South Surra, Kuwait (29°16'34.7"N 48°00'56.1"E) and was opened in 2018. The hospital area is 695,000 m^2 with 13 floors and two underground floors. The hospital houses 1,168 beds. The Temporary Quarantine Facility (TQF) is a separate building that is located in front of Jaber Hospital and was used to support the Ministry of Health when Jaber Hospital was fully occupied. The TQF has four floors comprising a total area of 12,531 m^2 and 85 patient rooms. During the sampling period, the TQF was used for swab testing and as a temporary location for COVID-19 patients.

In this study, Jaber Hospital and the TQF were the sole designated COVID-19 facilities in Kuwait. The Jaber Hospital only treated COVID-19 patients (patients with other ailments were treated elsewhere). All patients who had a positive reverse transcription polymerase chain reaction (RT-PCR) test were admitted to the hospital for quarantine, observation, and treatment. Because of this admission policy, even asymptomatic patients (those who tested positive but did not show any symptoms) were admitted to the hospital. Asymptomatic patients were discharged from the hospital only when they repeatedly tested negative on nasopharyngeal swabs.

3.1.2 Sample Locations

We conducted two sampling campaigns. The first campaign lasted from April 30 to May 20, 2020. The second campaign occurred between June 24 and July 10, 2020. The first campaign was only conducted at Jaber Hospital (inside and outside). Locations in the first campaign included ambient-pressure ICUs, inside rooms of symptomatic and asymptomatic patients with one to four beds, nearby nurses' workstations, inside a nurses' locker room, and at three different outside gates (Table C.1). The second campaign included Jaber Hospital (inside and outside), as well as locations inside and outside the TQF. Jaber Hospital locations during the second campaign included negative pressure ICUs, ambient pressure ICUs, bathrooms (2 m away from the toilet), observation rooms, and an outdoor gate. Locations at the TQF during the second campaign included a reception waiting area, COVID-19 swab testing waiting area, swab testing area exit, patient area hallway, and main entrance gate (Table C.2). We collected 84 samples in the first campaign from Jaber Hospital locations, 66 samples from the second campaign from Jaber Hospital locations, and 60 samples from the second campaign at the TQF (210 samples). We used a blank cascade for each collection period (36 total) and processed them simultaneously with the corresponding samples for that given period.

3.1.3 Sampling

We used custom-designed Harvard Micro-Environmental Cascade Impactors[39] to collect simultaneous samples in three distinct size fractions: fine (≤2.5 μm aerodynamic diameter), coarse (2.5-10 μm), and large (≥10 μm) (Figure 3.1). The first impactor stage used a polyurethane foam (PUF) substrate to collect large particles. The second impactor stage used a smaller PUF substrate to collect particles in the coarse size range. The last stage collected fine particles on a 37-mm diameter glass-fiber filter. For each sampling period, the impactor ran continuously for 48 h at a constant flow rate of 5 L/min, which corresponds to a total sampling volume of 14.4 m^3.

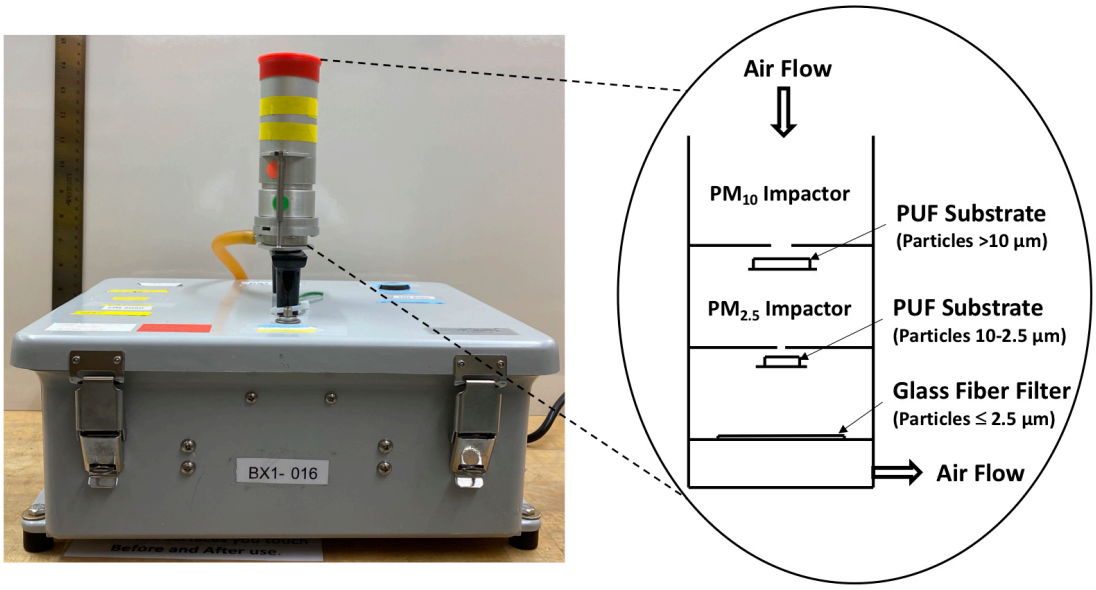

Figure 3.1: Micro-environmental cascade impactor designed and custom-built by the Environmental Chemistry Laboratory at the Harvard T.H. Chan School of Public Health (HSPH). PUF = polyurethane foam.

3.1.4 Post-sample processing

Following each sample collection, we processed the samplers in a biosafety level-2 laminar flow hood equipped with a high-efficiency particulate air (HEPA) filter. We aseptically removed the samples and transferred them into individual 5-mL sterile centrifuge tubes, submerged the substrates in RNAlater Stabilization Solution (Ambion, Inc., Austin, TX, USA), sealed the tubes with parafilm tape, and placed each tube inside an individual sterile Whirl-Pak (Whirl-Pak®, Nasco, USA) bag. We stored all samples and blanks at 4°C, and then shipped them overnight on ice to Molecular Research LP (Shallowater, Texas, USA).

3.1.5 RNA Extraction and reverse transcription quantitative polymerase chain reaction (RT-qPCR)

RNA extraction and RT-qPCR were performed at Molecular Research LP (Shallowater, Texas, USA). Viral RNA was extracted using the RNeasy Mini Kit (Qiagen, Hilden, Germany) following the manufacturer's instructions. Furthermore, 5.6 µg Poly-A carrier RNA (Qiagen, Hilden, Germany) was also mixed with each sample for extraction. Carrier RNA enhances the low copy viral nucleic acids binding to the mini column. In addition, it reduces the chance of viral RNA degradation. RNA was eluted in 40-µL RNase free water. RNA quantity and quality were determined using NanoDrop2000 (Thermo Scientific, Waltham, MA, USA). Samples were then used to quantify the viral concentrations by qPCR using 2019-nCoV CDC qPCR probe assays (Integrated DNA Technologies, Inc., Coralville, IA, USA) for the nucleocapsid N gene (Table C.3). 12 µL of RNA sample was first used for cDNA synthesis using QuantiTect Reverse Transcription kit (Qiagen, Hilden, Germany). 2 µL of the synthesized cDNA was used to perform the qPCR reaction using 2X PrimeTime Gene Expression Master Mix (Integrated DNA Technologies, Inc., Coralville, IA, USA) in StepOnePlus Real-Time PCR System (Applied Biosystems, Waltham, MA, USA). The

qPCR reaction was carried out with an initial holding stage of 95°C for 3 min for PCR enzyme activation. The cycling stage consisted of 45 cycles at 95°C for 5 s, followed by 55°C for 30 s. Genomic RNA from SARS-CoV-2 (2019-nCoV/USA-WA1/2020; ATCC, Manassas, VA, USA) was used as a standard. We identified positive samples as those below a cycle threshold of 39 (Table C.6).

3.1.6 Statistical analysis

We calculated the percent of positive samples by dividing the number of positive samples by the number of samples collected for each location category. The air concentrations of SARS-CoV-2 RNA copies are calculated by Equation 3.1:

$$C = p \cdot 20 \cdot e_v \div s_v \div v_{air} \tag{3.1}$$

where C = concentration (copies/m^3), p = copies/2μL cDNA estimated by PCR, e_v = extraction volume (μL), s_v= sample volume of storage liquid (μL), and v_{air} = volume of air collected (m^3). The copies/2 μL of cDNA from PCR were estimated using a standard curve. Adjustment by the factor of 20 was used to account for the fact that only 2 μL of cDNA were used out of the total 40 μL elution. We summarize sample concentrations (in copies/m^3) using the means and standard deviations of samples collected at any given location.

3.2 Results

We collected 210 samples during the study period. Out of the Jaber Hospital samples (150 samples total), 13 were positive (Table 3.1). Among the 13 positive samples, eight were detected at indoor locations and five were detected at the outside locations near the hospital entrance gates. Among the indoor locations, positive samples were observed in the ambient pressure ICUs (two positive samples) and in the rooms of multiple- and single-bed symptomatic patients (six positive samples). The

remaining indoor locations at Jaber Hospital (negative pressure ICU, asymptomatic patient rooms, nurse's workstations, nurse's locker room, staff bathrooms, hospital lobby, and observation rooms) had no positive samples. For the outdoor locations, we observed positive samples outside all three hospital entrances (Gates 1, 2, and 7). Gate 1 was used for suspected patients who visited the hospital for COVID-19 testing. Gate 2 was used for medical staff and visitors without symptoms. Gate 7 was used as an entrance for confirmed COVID-19 patients and ambulances bringing confirmed patients for hospitalization. All 60 samples at the TQF were negative for SARS-CoV-2 RNA (Table C.4). All blanks were negative for SARS-CoV-2 RNA.

Table 3.1: Number of positive samples detected in each location category by size fraction. TQF = Temporary Quarantine Facility.

	≤2.5 μm	2.5-10 μm	≥10 μm	TOTAL
ICU – Ambient Pressure	1	1	0	2
ICU – Negative Pressure	0	0	0	0
Symptomatic Patient Rooms	0	3	3	6
Asymptomatic Patient Rooms	0	0	0	0
Nurse's Stations	0	0	0	0
Nurse's Locker Room	0	0	0	0
Observation Rooms	0	0	0	0
Staff Bathrooms	0	0	0	0
Hospital Lobby	0	0	0	0
Outside Hospital Entrance Gates	2	3	0	5
TQF - Outside main gate	0	0	0	0
TQF - Swab exit	0	0	0	0
TQF - Swab waiting area	0	0	0	0
TQF - Reception waiting area	0	0	0	0
TQF - Patient area hallway	0	0	0	0
TOTAL	3	7	3	13

The fraction of positive samples was greatest for the symptomatic patient rooms (6 out of 24 samples or 25%) (Table C.5). The ambient-pressure ICU and outside the hospital gates had similar rates of positive samples (2 out of 21 or 10% for the ICU; 5 out of 33 or 15% for outside gates). None of the negative pressure ICU samples were positive.

In Figure 3.2, we present average concentrations of SARS-CoV-2 RNA across the location cate-

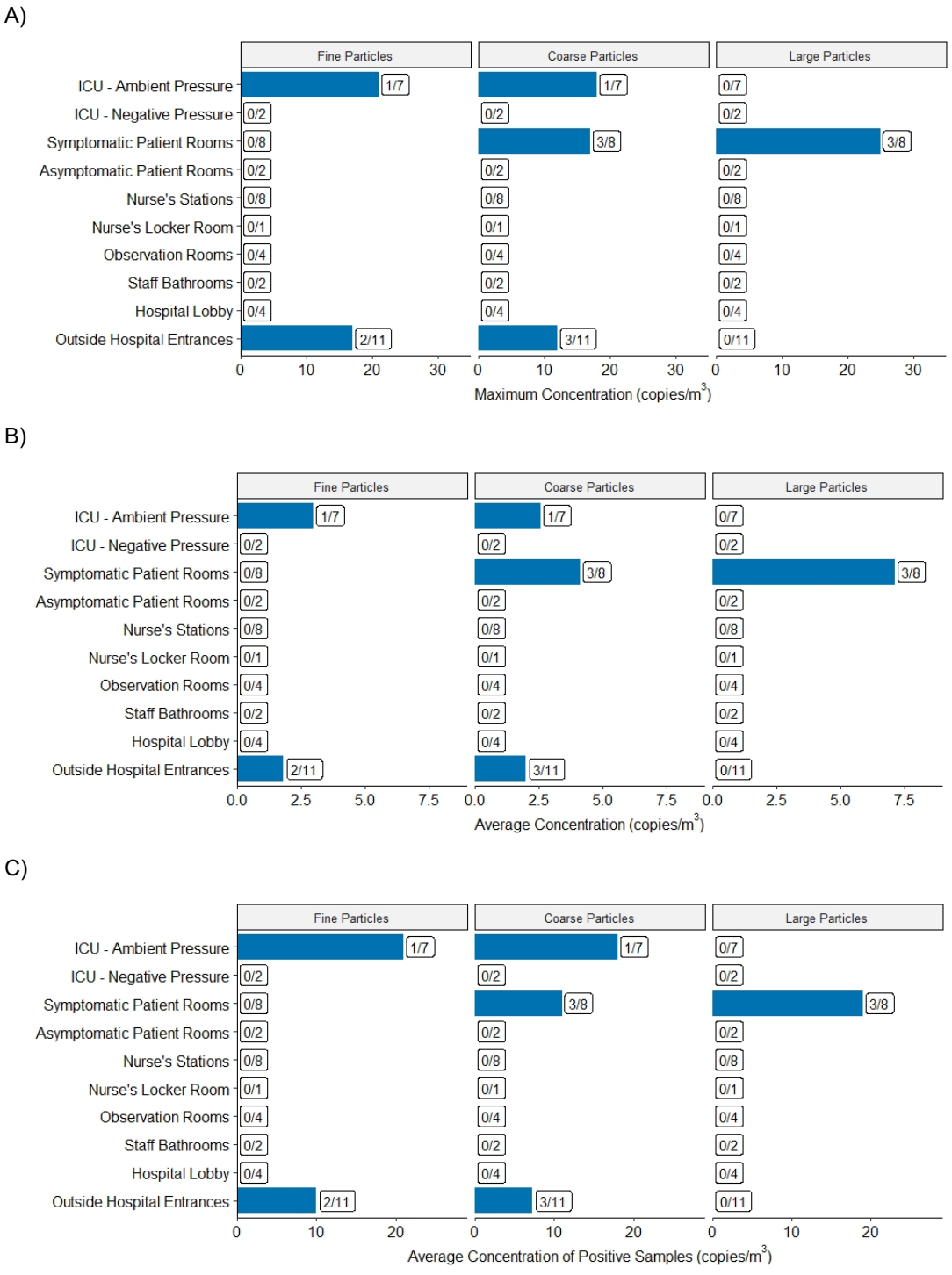

Figure 3.2: Concentration of SARS-CoV-2 RNA by sampling location category. (A) shows average concentration of all samples, including zero or non-detects; (B) shows average concentration of only the samples with positive or measurable concentrations; (C) shows maximum concentration among the positive samples when more than one positive sample was collected for a given location category. The boxes include the ratio of the number of positive samples to the total number of samples.

gories. Maximum concentrations in the rooms of symptomatic patients (25 copies/m^3) were higher than maximum concentrations in all other sampling locations (17-21 copies/m^3) (Figure 3.2; Table C.4). None of the samples in the rooms of asymptomatic patients were positive. Concentrations in the locations outside the hospital gates (3-17 copies/m^3) were relatively low compared to those in the symptomatic patient rooms (8-25 copies/m^3) and the ICUs (18-21 copies/m^3). Among the outdoor locations, Gate 7 had the highest viral concentration (17 copies/m^3 in the fine size fraction).

SARS-CoV-2 RNA was present in all three size fractions examined. The coarse size fraction had more positive samples (7 samples) than the fine (3 samples) or large (3 samples) sizes. In addition, the size distribution was dependent on the area in which the sample was collected (Table 1). Positive samples from symptomatic patient rooms were in the coarse (3 samples) and large (3 samples) size fractions. ICU samples were positive in the fine (1 sample) and coarse (1 sample) sizes. Outside the hospital gates had positive samples in the fine (2 samples) and coarse (3 samples) size fractions.

3.3 Discussion

The results comprise the largest dataset on size-fractionated airborne SARS-CoV-2 RNA to date. We collected 210 size-fractionated samples at Kuwait's designated COVID-19 inpatient state-of-the-art hospital and quarantine facility. We found positive samples in all three size fractions (fine ≤2.5 μm, coarse 2.5-10 μm, and large ≥10 μm). We confirmed our hypothesis, finding positives samples in the fine size fraction and in a pattern indicating location-specific size distributions.

A key finding is that the size distribution of particle-associated SARS-CoV-2 was related to the location where the particles were collected. Samples collected in symptomatic patient rooms were associated with larger particles, which may be because patients were not required to wear their masks at all times in their rooms. Symptomatic patients were also more likely to cough and sneeze, and both of these behaviors generate larger particles than speaking and breathing.[118] By contrast, all

samples collected in the asymptomatic patient rooms were negative. This could be because asymptomatic patients had a longer hospital stay than symptomatic patients, and therefore may have become less infectious over time.[167] This conclusion is also in agreement with Chia et al. (2020)[29], who reported that concentrations of the virus in air samples at hospital settings are highest in the first week of COVID-19 illness.

Positive samples in the ambient-pressure ICUs were in the fine and coarse sizes but not in the large size fraction, perhaps because these patients were intubated and unable to shed large particles through actions such as coughing and sneezing. Previous research indicates that exhaled particles from mechanically ventilated patients are between 0.3 μm and 1 μm, which is smaller than the large size fraction tested.[159] This size distribution agrees with our finding of SARS-CoV-2 RNA in the fine size fraction in the intubated patient rooms. It reinforces the importance of airborne personal protective gear for ICU healthcare workers that limits small particle exposure, especially for physicians and nurses attending to intubated patients. The emphasis on "droplet precautions" during patient intubation and extubation leads to an emphasis on large droplet routes but does not account for smaller aerosol precautions that could also prevent exposure.[164,175]

None of the negative pressure ICU sampling locations yielded positive results. The negative pressure precautions appeared to be effective at keeping airborne concentrations of the virus low or zero.[141,140,86] Engineering controls such as negative pressure could be challenging in some hospital environments that are already overwhelmed; yet, we show that these conditions appear to be effective.

Outdoor locations are considered to pose reduced risk for COVID-19 transmission compared to indoor locations due to greater dilution and UV exposure[113,127], so it was unexpected to find a similar percent of positive samples in the outside gate locations and the indoor ambient-pressure ICU. Positive samples in the outdoor locations were perhaps due to people nearby these locations being symptomatic, in close proximity, and emitting high viral loads. Positive samples from the outside

gates were in the fine and coarse size fractions. Emissions sources at the outside gates may be located farther from the sampler, thus producing particles at the smaller end of the spectrum. In addition, transport processes in outdoor air may select for smaller sizes due to evaporation and settling out of larger particles. Concentrations were higher at the gates with suspected and confirmed patients (Gate 7 and Gate 1) compared to Gate 2, which was designated for staff and visitors without symptoms. Gate 7, which was used for confirmed COVID-19 patients, had an even greater concentration and positive sample rate than Gate 2, which was used for suspected patients. Areas just outside the hospital – which may be thought to have reduced risk of exposure to the virus and where visitors promptly remove their masks – should perhaps be considered part of the hospital with respect to COVID-19 prevention and policies.

Numerous studies have detected SARS-CoV-2 RNA in airborne samples that collected total suspended particulate (TSP) air samples using a single, bulk sample without size fractionation.[138,42,82,11,84,129] Other studies collecting TSP did not find any SARS-CoV-2 RNA at all.[89,116,28,48,99] However, very few studies have collected size-fractionated samples. Liu et al. (2020)[92] and Chia et al. (2020)[29] collected three times each. Santarpia et al. (2020)[137] collected six times, Stern et al. (2021) collected 30 times[146], and Lednicky et al. (2020)[85] collected once. All of these studies found positive samples in multiple size fractions, which agrees with our results. Santarpia et al. (2020)[137] found SARS-CoV-2 RNA in <1, 1-4, and >4.1 μm sizes. Lednicky et al. (2020)[85] found SARS-CoV-2 RNA in all sizes examined except for the smallest one (<0.25 μm) inside a car driven by a COVID-19 patient. Chia et al. (2020)[29] found the virus in particles 1-4 μm and >4 μm size fractions inside COVID-19 patient rooms. Stern et al. (2021)[146] found SARS-CoV-2 RNA in particles ≤2.5, 2.5-10, and ≥10 μm inside a hospital.

Our finding of location-dependent size preferences for SARS-CoV-2 is supported by the results of Liu et al. (2020).[92] The authors found that smaller size fractions were associated with personal protective equipment (PPE) removal rooms and larger sizes were associated with medical staff of-

fices. However, Liu et al. (2020) found greatest concentrations near the toilet and PPE removal rooms.[92] By contrast, in the present study, we did not find any virus copies in the staff bathrooms or nurse's locker rooms. It appears that areas of greatest risk for exposure to airborne SARS-CoV-2 RNA may vary by hospital. Alternatively, the differences may simply be due to chance given the low number of positive samples were not sufficient for statistical analysis in either study.

The maximum concentration (25 copies/m^3) in our study was lower than those reported by previous studies (42 copies/m^3 for Liu et al. (2020)[92], 51 copies/m^3 for Stern et al. (2021)[146], and 2,000 copies/m^3 for Chia et al. (2020)[29]). There are many potential reasons that could explain this. First, there were methodological differences concerning proximity to the sampling device, RNA degradation, extraction efficiency from substrates, and PCR sensitivity. Second, the hospital settings were different. Jaber Hospital is a newly built, state-of-the-art facility that opened in 2018 with spacious rooms and hallways that are continuously disinfected. The hospital had very strict rules about limiting access and foot traffic. In comparison to hospitals in other studies[92,138], the Jaber Hospital is very large, which may have had dilution effects that further reduced levels of airborne virus. In the second campaign, all Jaber Hospital locations were negative, which may be partly explained by the decrease in foot traffic in the hospital, as during this campaign there were additional locations open for COVID-19 swab testing and hospitalization to reduce overcrowding. While hospital-specific practices, such as the maximum number of people allowed in the room at once and air exchange rate, may alter the risk of exposure, it is also imperative to acknowledge the potential uncertainty that is associated with the current study design, individual shedding, and location generalizability. Variability in emission rates from sources can vary by orders of magnitude.[96,24] Differences in maximum concentration between air sampling studies are likely to be explained by variability in environmental measures as well as individual variability in viral shedding.

This study has some limitations. First, the concentrations estimated in this study were time-weighted averages over 48-h sampling periods, and it is possible that the emissions of the virus into

the air occurred in discrete bursts rather than continuously over the entire sampling period. Thus, someone exposed may have received a higher 'dose' in the air than those implied based on the measured concentrations. Additionally, we were not able to obtain data on air exchange rates in the indoor sampling locations and therefore we could not assess the effects of ventilation on the presence of airborne SARS-CoV-2 or the number of viral copies in positive samples. The infectious dose of SARS-CoV-2 is still unknown. It is possible that it is similar to that of SARS-CoV-1,[7] which was estimated to require 280 viral particles to cause illness in 50% of people.[163] Further, given the sampling method, the present study did not measure viability of the virus, which would be necessary to determine whether SARS-CoV-2 is capable of causing infection. Previous studies have found SARS-CoV-2 to be viable in hospital air, including in particles <1 μm.[137,84] Finally, because of the low number of positive samples, we were not able to statistically test differences by location or size fractions.

3.4 Conclusion

While hospitals confront inevitable COVID-19 outbreaks among healthcare workers, a better understanding of the properties of airborne SARS-CoV-2 is essential to predict the spread of the disease in hospital settings. Providing the largest dataset of size-fractionated airborne SARS-CoV-2 RNA to date, we show that SARS-CoV-2 RNA is present with airborne particles of ≤2.5 μm, 2.5-10 μm, and ≥10 μm. The size distribution of the virus depended on the sampling location, which may be due to a combination of varying emission mechanisms, distance from the source, presence of symptomatic patients, and amount of human foot traffic. Hospital staff would benefit from considering location-specific features – including foot traffic, airflow, cleaning frequency, and patient status – when designing airborne prevention protocols. Airborne precautions, including those targeting fine particulate matter, seem to be a convincing strategy to protect healthcare workers from

the risk of COVID-19.

4

Conclusion

Interest has been growing in the field of aeromicrobiology with the discovery of diverse, abundant, and influential species in the atmospheric microbiome. This thesis described several contributions to the field of aeromicrobiology and environmental engineering. I investigated three key components about the airborne microbiome, which dictate their impact on environmental and human health: (1) What microbes are present; (2) Where they are located; and (3) How they spread.

In Chapter 1, I presented the first ever cultivation-independent data on the airborne microbiome in Mali, West Africa. I found abundant and diverse microbes in all particle sizes at levels higher than those previously hypothesized for desert regions. This finding is important given projected future

desertification and the increased frequency of desert dust storms spreading particle-borne microbes over long distances. In fact, I found similarities between members of the airborne microbiome in the Sahara and in destinations such as Europe following long-distance transport of Saharan dust. Our finding of abundant and diverse taxa on fine particles (≤2.5 μm) was significant given that fine particles can travel farther and penetrate deeply into the lungs. Finally, I revealed the presence of four potential pathogens using PCR that would be candidates for future viability tests. Three of the four species were detected with particles ≤2.5 μm, indicating the potential for long-distance transport and penetration into the lungs and bloodstream.

In Chapter 2, I presented the use of a custom-built compact cascade impactor for surveillance of airborne SARS-CoV-2 RNA at locations inside a Boston hospital. I showed that positive samples were more likely to be found in non-COVID-19 designated areas that in the COVID-19 wards. This highlights the need for universal precautions against airborne spread of the disease and suggests effectiveness of measures such as negative pressure. All three size fractions tested (≤2.5, 2.5-10, and ≥10 μm) had about the same frequency of positive detection of SARS-CoV-2 RNA. Presence in fine (≤2.5 μm) particulate matter suggested the potential for an airborne residence time on the order of hours, depending on air filtration and exchange rates, with a potential spread distance of farther than six feet and penetration of the virus deep into the lungs.

Chapter 3 described one of the most comprehensive size-fractionated studies of airborne SARS-CoV-2 to date. In contrast to the study in Chapter 2, I found a location-dependent size distribution for SARS-CoV-2 RNA. Larger particles ≥10 μm with the virus were most abundant in symptomatic patient rooms, which may be explained by reduced mask wearing inside the rooms and symptomatic behaviors like coughing that produce larger particles containing the virus. Fine particles ≤2.5 μm were more frequently detected in the rooms of intubated patients and outside the hospital entrance gates. Universal PPE precautions that protect against fine particles – not just large droplets – are critical. These precautions should be applied stringently in non-COVID-19 locations

as well as COVID-19 designated care areas. Outstanding questions remain regarding extraction efficiency from sampling substrates, optimization of the SARS-CoV-2 RT-PCR assay, and infectious dose of SARS-CoV-2 following inhalation. Zero values in samples in Chapters 2 and 3 had a large uncertainty attached to them, and the limit of detection of the assay and viral particle losses due to sample processing may be substantial. Understanding the limit of detection for each methodology is important for evaluating the true risk of exposure to airborne microbes including SARS-CoV-2.

This dissertation was motivated by a passion for understanding the presence and impact of airborne microbes on human health. As the technologies for identifying microorganisms continue to develop, it is critical that scientists from engineering, microbiology, and aerosol science come together to continue advancing this field. Through interdisciplinary collaboration, we will be able to unfurl the stunning diversity of the airborne microbiome.

A

Supporting Information for Chapter 1

Table A.1: Average meteorological conditions on sampling days at the collection site in Bamako, Mali (Lat 12.332 N, Lon -7.578 W).

Date	Sampling Day	Wind speed (m/s)	Relative humidity (%)	Majority wind direction	Air temperature (°C)	Barometric pressure (mm Hg)
Feb. 11, 2018	1	1.51	6.1	NNE	30.3	29.87
Feb. 13, 2018	2	1.23	6.5	NNE	33.5	29.86
Feb. 14, 2018	3	0.99	4.8	NE	35.1	29.84
Feb. 15, 2018	4	1.41	2.6	NNE	36.0	29.87
Feb. 16, 2018	5	1.41	2.0	ENE	37.1	29.89
Feb. 17, 2018	6	1.26	4.2	NNE	37.3	29.83
Feb. 18, 2018	7	1.25	4.0	NNE	39.1	29.78
Feb. 19, 2018	8	1.14	10.3	NE	38.2	29.75
Feb. 20, 2018	9	1.58	9.4	NNE	33.0	29.79

Table A.2: Samples tested for species with known pathogenic strains using PCR.

Pathogen target	Sample Tested	Particle Size (μm)	+ / -
Bacillus cereus	D2.C.F	<0.5	+
	D3.C.F	<0.5	+
	D7.C.P1	2.5-1.0	-
Escherichia coli	D3.C.F	<0.5	+
	D3.C.P1	2.5-1.0	-
	D9.C.P0.5	1.0-0.5	+
Fusobacterium nucleatum	D6.C.P1	2.5-1.0	+
	D3.C.P0.5	1.0-0.5	-
	D9.C.F	<0.5	-
	D4.C.P2.5	10.0-2.5	+
Streptococcus pneumoniae	D3.C.P0.5	1.0-0.5	-
Staphylococcus epidermidis	D9.C.P2.5	10.0-2.5	-
	D8.C.P1	2.5-1.0	-
	D5.C.P0.5	1.0-0.5	-
	D4.C.P1	2.5-1.0	-
Pseudomonas aeruginosa	D3.C.P2.5	10.0-2.5	+

Table A.3: Primer set sequences for PCR of potential pathogens.

Species	Primer sequence
Escherichia coli	EcoliuidA_FPrimer:CGGAAGCAACGCGTAAACTC EcoliuidA_RPrimer: TGAGCGTCGCAGAACATTACA EcoliuidA_Probe:/56-FAM/CGCGTCCGATCACCTGCGTC/ 3BHQ_1/
Pseudomonas aeruginosa	pseuF: ACTTTAAGTTGGGAGGAAGGG pseuR: ACACAGGAAATTCCACCACCC pseuProbe: Fam-ACAGAATAAGCACCGGCTAAC-BHQ
Streptococcus pneumoniae	Sp-lytAF: ACG CAA TCT AGC AGA TGA AGC A Sp-lytAR: TCG TGC GTT TTA ATT CCA GCT Sp-lytAP: /56-FAM/CCGAAAACGCTTGATACAGGGAG/ 3BHQ_1/
Staphylococcus epidermidis	StaphepiF: ACTGGTTACCCTGGTGACAAACCA StaphEpiR: ACTGGAGATCCAGAGTTTCCACCT staphepiProbe: /56-FAM/AGCCACAATGTGGGAAAGTGTAGGT/ 3BHQ_1/
Bacillus cereus	bacCereusF: CTGTAGCGAATCGTACGTATC bacCereusR: TACTGCTCCAGCCACATTAC bacCereusP: /56-FAM/GGAGCTGTACAACTTGCCA/3BHQ_1/
Fusobacterium nucleatum	FnucleatF-R-P: proprietary

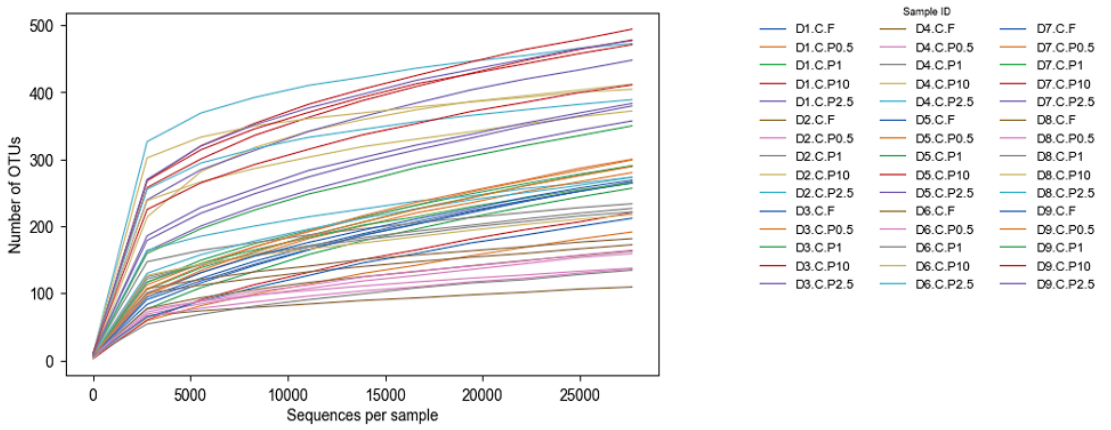

Figure A.1: Rarefaction curves of operational taxonomic units (OTUs) clustered at 99% sequence identity across all samples.

Table A.4: Taxonomic assignment for operational taxonomic units (OTUs) that differed significantly across the various particle sizes and the particle size fraction with greatest abundance.

Taxonomic Assignment	Particle size preference (µm)
p__Actinobacteria; c__Actinobacteria; o__Actinomycetales; f__Geodermatophilaceae; g__Geodermatophilus; s__obscurus	>10.0
p__Firmicutes; c__Bacilli; o__Lactobacillales; f__Aerococcaceae; g__; s__	10.0-2.5
p__Firmicutes; c__Clostridia; o__Clostridiales; f__Ruminococcaceae; g__; s__	>10.0
p__Actinobacteria; c__Actinobacteria; o__Actinomycetales; f__Intrasporangiaceae	10.0-2.5
p__Actinobacteria; c__Actinobacteria; o__Actinomycetales; f__Intrasporangiaceae	10.0-2.5
p__Firmicutes; c__Clostridia; o__Clostridiales; f__Ruminococcaceae; g__; s__	>10.0
p__Firmicutes; c__Bacilli; o__Bacillales; f__Planococcaceae	2.5-1.0
p__Actinobacteria; c__Actinobacteria; o__Actinomycetales; f__Corynebacteriaceae; g__Corynebacterium; s__	2.5-1.0
p__Actinobacteria; c__Actinobacteria; o__Actinomycetales; f__Geodermatophilaceae; g__Geodermatophilus; s__obscurus	>10.0
p__Actinobacteria; c__Actinobacteria; o__Actinomycetales; f__Nocardioidaceae; g__; s__	10.0-2.5
p__Actinobacteria; c__Actinobacteria; o__Actinomycetales; f__Corynebacteriaceae; g__Corynebacterium; s__	2.5-1.0
p__Proteobacteria; c__Alphaproteobacteria; o__Rhizobiales; f__Bradyrhizobiaceae; g__Balneimonas; s__	10.0-2.5
p__Proteobacteria; c__Gammaproteobacteria; o__Pseudomonadales; f__Moraxellaceae; g__Psychrobacter; s__pulmonis	>10.0
p__Actinobacteria; c__Actinobacteria; o__Actinomycetales	>10.0

A.1 Additional Text: Difference in bacterial diversity across particle sizes

Additional details on genera detected and corresponding potential sources are presented in Additional Text Table A.5. At the genus level, *Geodermatophilus*, a soil-associated genus, was more abundant in the largest (>10 μm) size fraction (Kruskal-Wallis test, FDR $p < 0.05$). Prior work found strains of *Geodermatophilus* in 1-2 mm sand from the Saharan desert,[37] consistent with detection in this study preferentially on the largest particle sizes. The *Ruminococcaceae* family exhibited a preference for the largest particle size fraction (Kruskal-Wallis, FDR $p < 0.05$). This family was previously identified as an indicator for bovine fecal contamination.[19] The family *Dermatophilaceae*, which are common on animal and human skin, were most abundant in the largest two size fractions. Our sampling location was 11 km downwind of a cattle market, which could be a source of large, locally generated particles with distinct microbial composition.

One taxonomic class (Thermomicrobia) out of the 62 classes detected statistically differed among the five atmospheric particle sizes (Kruskal-Wallis test, FDR $p < 0.05$), with greatest abundance in the particle size range of 10.0-2.5 μm. This class has been found in a wide range of soil types, typically isolated from human activity.[72] Thermomicrobia were previously found in the desert soil of the Sahara[8], indicating the potential for local sources with larger particles that did not yet fall out due to gravitational settling.

Table A.5: Additional Text Table. Genera detected in the samples and corresponding potential sources.

Soil	Skin	Stool	Compost	Wastewater Treatment	Land Application Biosolids
Bradyrhizobium *Mesorhizobium*	*Propionbacterium* *Staphylococcus* *Corynebacterium* *Streptococcus* *Rothia* *Micrococcus* *Anaerococcus* *Brevibacterium*	*Bacteroides* *Faecalibacterium* *Oscillospira* *Roseburia* *Coprococcus* *Ruminococcus* *Parabacteroides* *Phascolarctobacterium* *Sutterella* *Blautia*	*Saccharopolyspora*	*Arcobacter*	*Clostridium*

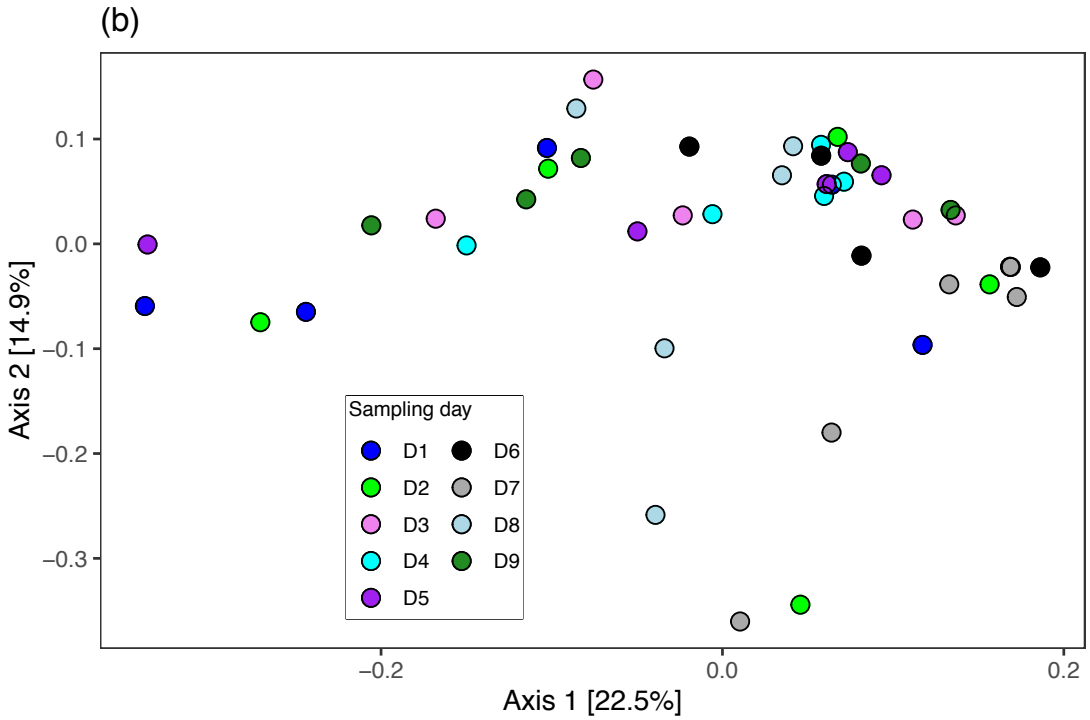

Figure A.2: Community analysis using pairwise, weighted UniFrac distances visualized on a principal coordinates analysis (PCoA) plot with the percent of variation explained by each axis noted in brackets. Samples were grouped by sampling day.

Table A.6: Taxa detected with features for survival in harsh atmospheric conditions.

Taxa detected in the samples	Relevant trait
Burkholderiales, Pseudomonadales, Flavobacteriales	Common in outdoor air [126]
Bacillaceae	Forms endospores
Gemmatimonadetes, Thermus, Chloroflexi, *Psychrobacter*, Myxococcales	Commonly found in extreme environments
Gemmatomonadetes, *Deinococcus*	Associated with hyper-arid environments; bioindicators for Saharan dust events [49,104,31]
Gemmatomonadetes	UV protection during aerial transport due to carotenoid pigmentation [152,68]
Methylobacterium, Rubrobacter	Possess structures to resist environmental stresses [49,64]
Arthrobacter, Methylobacterium	Dessication-resistant [49]
Bacillus, Kocuria, Micrococcus	Detected in culture-based air samples in Mali [81]
Bacteroidetes	Preference for desert soils
Cytophagaceae (Hymenobacter), Flavobacteriaceae	Pigmented and psychrotolerant; previously found in Saharan dust [52]

Table A.6 Continued:

Nocardioides, Sporichthya, Beijerinckiaceae, Hyphomicrobiaceae, Acetobacteraceae, Skermanella, Rhodocyclaceae, Rhodospirillaceae, Sphingomonadaceae	Motile spores
Mesorhizobium	Motile by symbiosis with plant roots
Patulibacter, Rhodobacteraceae, Modestobacter	Psychrotolerance aids survival in Sahara at night[49]
Rubrobacteraceae, Streptosporangiaceae, Pseudonocardia, Rubellimicrobium, Streptomyces	Heat tolerant and thermophilic[49,58]
Rubrobacter, Hymenobacter, Methylobacterium	Gamma radiation-resistant[49,58]
Bacillus, Paenibacillus, Arthrobacter, Cellulomonas, Janthinobacterium, Modestobacter, Pseudomonas, Sphingomonas	UV resistant[151]
Nocardioides Halophilic Bacillaceae, Paenibacillaceae, Bacillus	Spore-forming
Geodermatophilaceae, Pseudonocardiaceae, Rhodocyclaceae, Rubrobacteraceae	oligotrophic
Frankia, Beijerinckiaceae, Bradyrhizobiaceae, Rhizobium, Rhizobiaceae, Mesorhizobium, Azospirillum, Rhodospirillaceae, Frankia, Oxalobacteraceae	Nitrogen-fixing

Table A.6 Continued:

Methylobacterium	convert nitrogen gas to ammonia and feed on methanol
Hyphomicrobiaceae	phototrophic
Rhodobacteraceae, Rhodocyclaceae, Rhodospirillaceae, Sphingomonas (aerobic)	Photoheterotrophic
Cellulosimicrobium, Actinobacteria	biodegrade cellulose or lignin
Cytophagaceae	Capable of degrading plant material
Clostridiaceae, Fusobacteriaceae, Lactobacillaceae, Oxalobacteraceae, Rhodospirillaceae	Strict anaerobes
Enterobacteriaceae, Myxococcaceae, Rhodospirillaceae	Facultative anaerobes
Methanobacteriales	thermophilic anaerobic methanogens

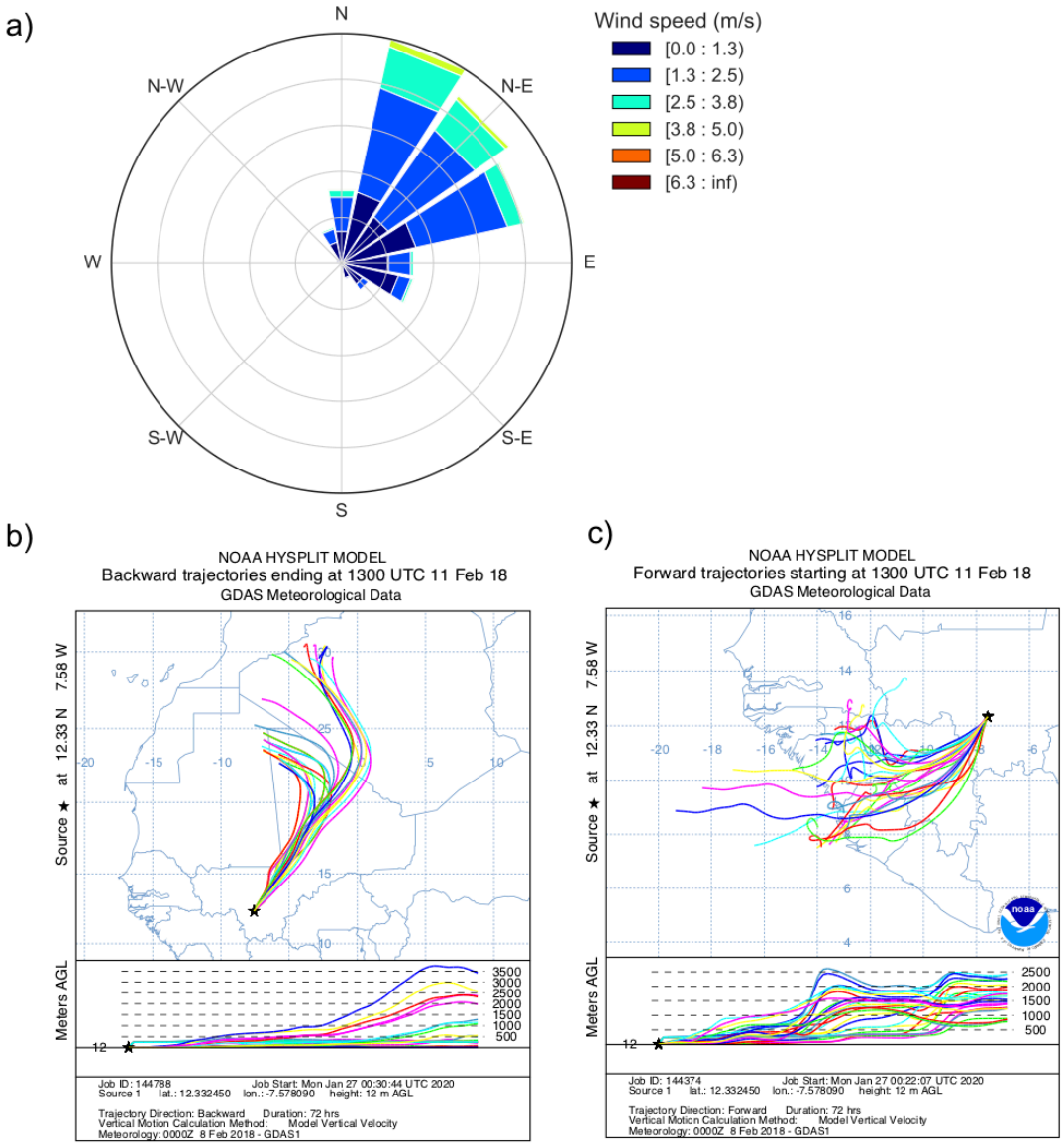

Figure A.3: (a) Wind direction and wind speed for sampling day 1 (Feb. 11, 2018); (b) HYSPLIT 72-hour backward trajectories from the sampling site for sampling day 1; (c) HYSPLIT 72-hour forward trajectories from the sampling site for sampling day 1. All other sampling days exhibited wind patterns and trajectories similar to sampling day 1 (Figure A.4).

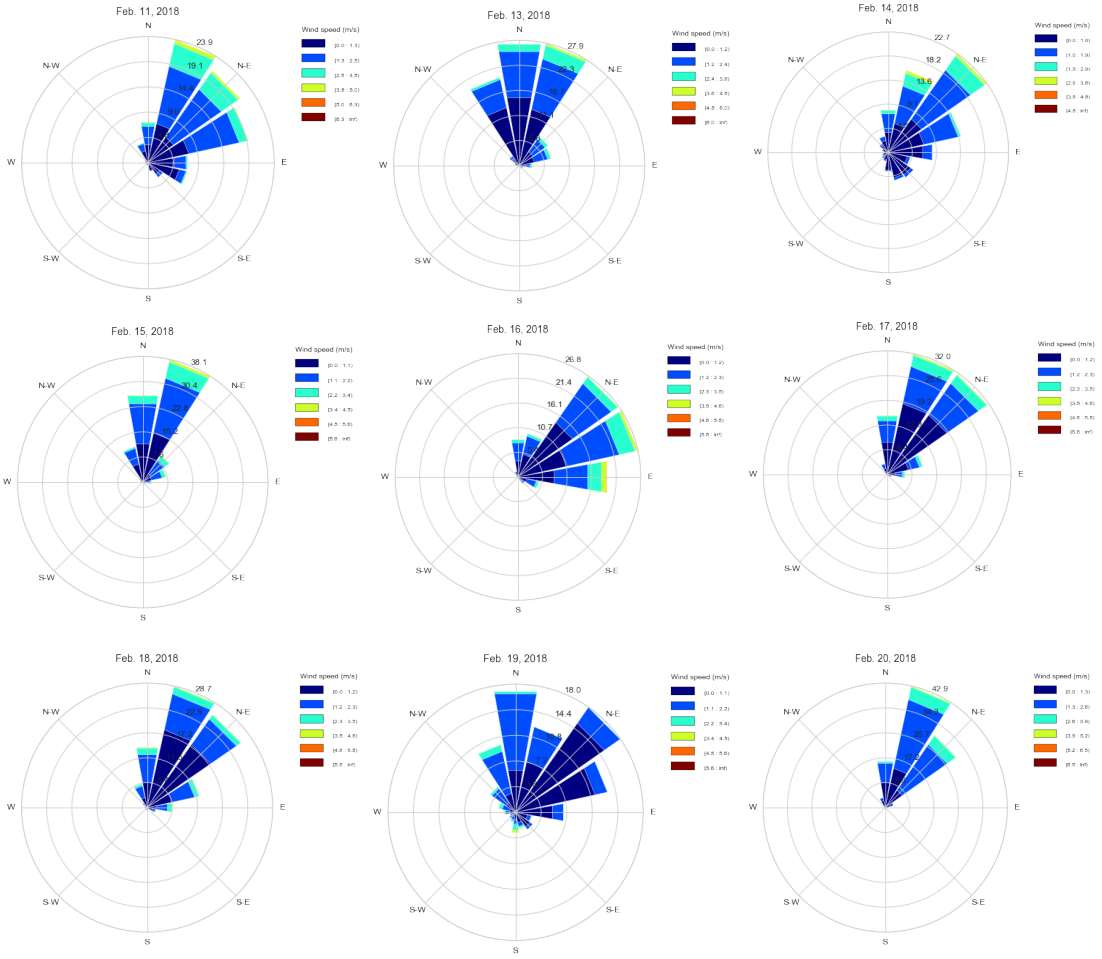

Figure A.4: Wind rose plots of instantaneous wind direction and velocity (m s^{-1}) during each of the sampling days reveal the winds were predominantly from the northeast.

B

Supporting Information for Chapter 2

Table B.1: Primers and probes used to target the nucleocapsid N gene.[155]

Name	Description	Oligonucleotide Sequence (5'>3')
2019-nCoV_N1-F	2019-nCoV_N1 Forward Primer	GAC CCC AAA ATC AGC GAA AT
2019-nCoV_N1-R	2019-nCoV_N1 Reverse Primer	TCT GGT TAC TGC CAG TTG AAT CTG
2019-nCoV_N1-P	2019-nCoV_N1 Probe	FAM-ACC CCG CAT TAC GTT TGG TGG ACC-BHQ1
2019-nCoV_N1-P	2019-nCoV_N1 Probe	FAM-ACC CCG CAT /ZEN/ TAC GTT TGG TGG ACC-3IABkFQ
2019-nCoV_N2-F	2019-nCoV_N2 Forward Primer	TTA CAA ACA TTG GCC GCA AA
2019-nCoV_N2-R	2019-nCoV_N2 Reverse Primer	GCG CGA CAT TCC GAA GAA
2019-nCoV_N2-P	2019-nCoV_N2 Probe	FAM-ACA ATT TGC CCC CAG CGC TTC AG-BHQ1
2019-nCoV_N2-P	2019-nCoV_N2 Probe	FAM-ACA ATT TGC /ZEN/ CCC CAG CGC TTC AG-3IABkF

Table B.2: Patients in the emergency department (ED) and probability of a positive sample in the ED.

Sampling Date	Total Respiratory Patients Evaluated in ED	Total ED Patients	Probability of a Positive Sample in ED
April 29-May 1, 2020	12	55	0/3
May 5-May 7, 2020	12	52	1/3
May 11-May 13, 2020	22	63	0/3
May 13-May 15, 2020	15	50	1/3
May 18-May 20, 2020	20	64	0/3
May 20-May 22, 2020	12	49	0/3

B.1 Sampling Location Details

Samplers were located: (1) in a corridor seven feet from the door to a negative pressure COVID-19 medical ward, (COVID-19 Ward 1, CW1); (2) in a 15-by-8 foot personal protective equipment (PPE) donning room located outside the entrance to a second negative pressure COVID-19 medical ward, directly in front of a station where persons put on PPE, including gowns, N95 masks, face shields, and shoe and head coverings (COVID-19 Ward 2, CW2); (3) in a corridor five feet from the entrance to the medical intensive care unit (requiring passage through a PPE donning room under negative pressure), (Intensive Care Unit, ICU); (4) a staff work station (an open area) of the emergency department eight feet from the entrance to two negative pressure rooms used for suspect COVID-19 patients (Emergency Department, ED), and; (5) at the staff work station of a ward that did not care for known COVID-19 patients (Non-COVID-19 Ward, NCW). This nurse's station was in an open area with the nearest potential COVID-19 patients (up to 6 suspected patients) down a corridor with entry doors 25 feet away. Midway through the study period (on May 12-18, 2020), CW1 was closed and cleaned, then opened as a non-COVID-19 ward. This new ward included a negative pressure unit that cared for suspected COVID-19 patients in a smaller wing distant from the entrance.

B.2 Sample Collection Details

The cascade impactors were cleaned with 70% alcohol and assembled and disassembled aseptically inside a biosafety level 2 (BSL2) laminar flow hood. Subsequently, the cascades were attached to the top of the pump box (see Figure 2.1). The sampling assemblies were sealed in plastic bags and transported aseptically to the hospital for sample collection. After sample collection, assemblies were sealed in plastic bags, and shortly thereafter were transported to and placed inside the BSL2 hood. Then, the cascade and pump box assemblies were removed from the plastic bags, cascades were detached from the box, and all box surfaces were sanitized with 70% ethanol. All personnel involved in sample collection, instrument setup and calibration, and sample processing wore personal protective equipment.

B.3 Shotgun Sequencing

B.3.1 Methods

One sample (VA-027-GFF) was selected at random out of the samples that amplified in PCR for shotgun sequencing to further assess the presence of SARS-CoV-2 RNA. The sample chosen was collected in the Emergency Department in the smallest particle size fraction on May 20-22, 2020. RNA quantity and quality were determined using a NanoDrop2000 (Thermo Scientific, USA). 5 uL of RNA sample was first used for cDNA synthesis using QIAseq SARS-CoV-2 Primer Panel kit (Qiagen) followed by PCR using 2 pools of SARS-CoV-2 Primers. The PCR reaction was carried out with an initial holding stage of 98°C for 2 minutes and 35 cycles of 98°C for 20 seconds, followed by 65°C for 5 minutes for annealing and extension. The PCR products obtained from 2 pools were pooled and purified using 1X PCR Clean DX beads (Aline Biosciences). The concentration of purified amplicon was evaluated using the Qubit dsDNA HS Assay Kit (Life Technologies). The library was prepared using QIAseq FX DNA Library kits (Qiagen) following the manufacturer's user guide. 10 ng of purified amplicon was used to prepare the library. The sample underwent the fragmentation, end repair and A-addition followed by adapter ligation with unique indices. Library was amplified using adapter specific primers by following the manufacturer's user guide. Following the library preparation, the final concentration of the library was measured using the Qubit dsDNA HS Assay Kit (Life Technologies), and the average library size was determined using the Agilent 2100 Bioanalyzer (Agilent Technologies). The library diluted (to 0.6nM) and sequenced paired end for 500 cycles using the NovaSeq system (Illumina).

B.3.2 Results

The sequenced SARS-CoV-2 RNA in sample VA-027-GFF was submitted to GenBank[32] with accession number MW047086. Analysis via NextStrain[66] produced multiple (conflicting) clade assignments, which suggests at least two distinct strains of SARS-CoV-2 in the sample. Sample VA-027-GFF previously had evidence of PCR amplification with a cycle threshold of 41.76, but it was above the 40.85 cutoff for positive samples that was determined based on the standard curve and a threshold of one copy of the virus per one microliter. Detection of SARS-CoV-2 in a sample that was near the PCR cycle threshold cutoff suggests that the detection of SARS-CoV-2 could have been underestimated in other samples.

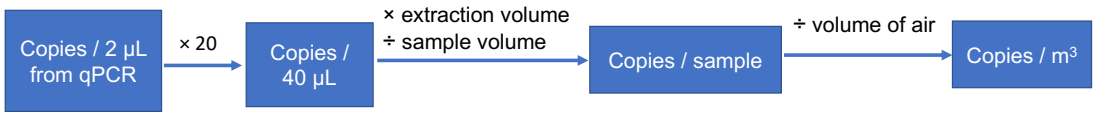

Figure B.1: Method for calculating copies/m^3 from the qPCR copy number. A standard curve was used to estimate the number of copies per 2 µL of cDNA used in qPCR.

C

Supporting Information for Chapter 3

Table C.1: Inside and outside sampling locations from Jaber Hospital (first campaign, April 30-May 20, 2020).

Indoor Sampling Locations	**Outdoor Sampling Locations**
ICUs (ambient pressure)	Gate 1 – Used for suspected and symptomatic patients
Multiple beds (≥ 4 beds) – Symptomatic patients	Gate 2 – Used for regular staff (i.e., doctors, nurses) and visitors
Multiple beds (≥ 4 beds) – Non-symptomatic patients	Gate 7 – Used for ambulance entrance and confirmed cases
Single bed – Symptomatic patients	
Nursing stations – Wards	
Nursing stations – ICUs	
Nurse's locker room	

Table C.2: Inside and outside sampling locations from both Jaber Hospital and the Temporary Public Quarantine (TQF) (second campaign, June 24-July 10, 2020).

Jaber Hospital	
Indoor Sampling Locations	**Outdoor Sampling Locations**
ICUs (negative pressure)	Gate 7 – Used for ambulance entrance and confirmed cases
ICUs (ambient pressure)	
Staff bathroom	
Reception (observation waiting area for suspected patients)*	
Reception observation room entrance (hallway)	
Observation room entrance (hallway)	
Temporary Public Quarantine (TQF)	
Indoor Sampling Locations	**Outdoor Sampling Locations**
Reception waiting area	Main gate entrance
Swab testing waiting area†	Swab testing exit
Patient hallway area‡	

*Sampler was put in various locations in reception: front, back, and center of reception waiting area
†Sampler was put in two locations in the Swab testing waiting area: in the front and back of waiting area
‡Sampler was put in two locations in the patient area hallway: in the right and left of the hallway

Table C.3: Primers and probes used to target the nucleocapsid N gene[155]

Name	Description	Oligonucleotide Sequence (5'>3')
2019-nCoV_N1-F	2019-nCoV_N1 Forward Primer	GAC CCC AAA ATC AGC GAA AT
2019-nCoV_N1-R	2019-nCoV_N1 Reverse Primer	TCT GGT TAC TGC CAG TTG AAT CTG
2019-nCoV_N1-P	2019-nCoV_N1 Probe	FAM-ACC CCG CAT TAC GTT TGG TGG ACC-BHQ1
2019-nCoV_N1-P	2019-nCoV_N1 Probe	FAM-ACC CCG CAT /ZEN/ TAC GTT TGG TGG ACC-3IABkFQ
2019-nCoV_N2-F	2019-nCoV_N2 Forward Primer	TTA CAA ACA TTG GCC GCA AA
2019-nCoV_N2-R	2019-nCoV_N2 Reverse Primer	GCG CGA CAT TCC GAA GAA
2019-nCoV_N2-P	2019-nCoV_N2 Probe	FAM-ACA ATT TGC CCC CAG CGC TTC AG-BHQ1
2019-nCoV_N2-P	2019-nCoV_N2 Probe	FAM-ACA ATT TGC /ZEN/ CCC CAG CGC TTC AG-3IABkF

Table C.4: Concentration of SARS-CoV-2 (copies m^{-3}) for each location category for Campaign 1 and Campaign 2. TQF = Temporary Quarantine Facility. Semicolon (;) indicates multiple samples. F = fine (≤2.5 μm); C = coarse (2.5-10 μm); L = large (≥10 μm)

Location	Size	Campaign 1						Campaign 2						
		4/30-5/2	5/2-5/11	5/11-5/13	5/14-5/16	5/16-5/18	5/18-5/20	6/24-6/26	6/26-6/28	6/28-6/30	6/30-7/2	7/4-7/6	7/6-7/8	7/8-710
		1	**2**	**3**	**4**	**5**	**6**	**7**	**8**	**9**	**10**	**11**	**12**	**13**
Symptomatic	F	0;0			0;0	0;0	0;0							
	C	0;0			0;0	8;17	8;0							
	L	0;0			0;12	25;0	20;0							
Asymptomatic	F			0;0										
	C			0;0										
	L			0;0										
Nurse's Station	F	0		0	0	0		0	0	0	0			
	C	0		0	0	0		0	0	0	0			
	L	0		0	0	0		0	0	0	0			
ICU	F		0	21	0	0	0			0	0			
	C		0	0	18	0	0			0	0			
	L		0	0	0	0	0			0	0			
Outside	F		3;0	0	0;0	0;0	17	0	0	0				
	C		0;3	0	0;0	0;7	12	0	0	0				
	L		0;0	0	0;0	0;0	0	0	0	0				
Nurse's Locker Room	F						0							
	C						0							
	L						0							
Lobby	F							0	0	0	0			
	C							0	0	0	0			
	L							0	0	0	0			
Observation - patient room	F							0	0	0	0			
	C							0	0	0	0			
	L							0	0	0	0			
ICU - negative pressure	F							0	0					
	C							0	0					
	L							0	0					
Outside - TQF	F							0	0	0	0	0	0	
	C							0	0	0	0	0	0	
	L							0	0	0	0	0	0	
Swab - TQF	F										0	0;0	0;0	0;0
	C										0	0;0	0;0	0;0
	L										0	0;0	0;0	0;0
Reception - TQF	F											0	0	0
	C											0	0	0
	L											0	0	0
Patient Hallway - TQF	F											0	0	0
	C											0	0	0
	L											0	0	0
Toilet	F												0	0
	C												0	0
	L												0	0

Table C.5: Positive samples, fraction of positive samples, and concentration summary for each location category.

			Concentration, mean (SD) (copies/m^3)		
	Number of positive samples / total number of samples	**Percentage of Positive Samples (%)**	**Fine (≤2.5 μm)**	**Coarse (2.5-10 μm)**	**Large (≥10 μm)**
ICU - Ambient Pressure	2/21	10	3.0 (7.9)	2.6 (6.8)	-
ICU - Negative Pressure	0/6	0	-	-	-
Symptomatic Patient Rooms	6/24	25	-	4.1 (6.3)	7.1 (10.4)
Asymptomatic Patient Rooms	0/6	0	-	-	-
Nurse's Stations	0/8	0	-	-	-
Nurse's Locker Room	0/3	0	-	-	-
Observation Rooms	0/12	0	-	-	-
Bathrooms	0/6	0	-	-	-
Hospital Lobby	0/12	0	-	-	-
Outside Hospital Entrances	5/33	15	1.8 (5.1)	2.0 (4.0)	-
TQF Outside main gate	0/18	0	-	-	-
TQF Swab	0/12	0	-	-	-
TQF Swab waiting area	0/9	0	-	-	-
TQF Reception waiting area	0/9	0	-	-	-
TQF Patient area hallway	0/9	0	-	-	-

Table C.6: Details and cycle threshold (CT) values for positive samples collected at Jaber Hospital.

Date	Location	Particle Size (μm)	Cт
May 2 to May 11	Outdoor Gate 2, medical staff and visitors' entrance	≤2.5	38.39
May 2 to May 11	Outdoor Gate 7, suspected and confirmed patients; ambulance entrance	2.5-10	37.68
May 11 to May 13	ICU Room A	≤2.5	38.22
May 14 to May 16	Symptomatic Patient Room A (4 beds, 4 patients)	≥10	38.75
May 14 to May 16	ICU Room B	2.5-10	37.49
May 16 to May 18	Symptomatic Patient Room B (4 beds, 4 patients)	2.5-10	38.81
May 16 to May 18	Symptomatic Patient Room B (4 beds, 4 patients)	≥10	37.65
May 16 to May 18	Symptomatic Patient Room A (4 beds, 4 patients)	2.5-10	37.58
May 16 to May 18	Outdoor Gate 1, suspected patients' entrance	2.5-10	38.88
May 18 to May 20	Symptomatic Patient Room C (1 bed, 1 patient)	2.5-10	38.83
May 18 to May 20	Symptomatic Patient Room C (1 bed, 1 patient)	≥10	37.93
May 18 to May 20	Outdoor Gate 7, suspected and confirmed patients; ambulance entrance	≤2.5	38.57
May 18 to May 20	Outdoor Gate 7, suspected and confirmed patients; ambulance entrance	2.5-10	38.16

References

[1] Akani, N. P., Hakam, I. O., & Sampson, T. (2019). Prevalence and Antibiogram of Pseudomonas aeruginosa Isolated from West African Mud Creeper (Tympanotonus fuscatus). *South Asian Journal of Research in Microbiology*, 5(2), 1–8.

[2] Apprill, A., McNally, S., Parsons, R., & Weber, L. (2015). Minor revision to V4 region SSU rRNA 806R gene primer greatly increases detection of SAR11 bacterioplankton. *Aquatic Microbial Ecology*, 75(2), 129–137.

[3] Asadi, S., Wexler, A. S., Cappa, C. D., Barreda, S., Bouvier, N. M., & Ristenpart, W. D. (2019). Aerosol emission and superemission during human speech increase with voice loudness. *Scientific Reports*, 9(1), 1–10.

[4] Asano, Y., Iwayama, S., Miyata, T., Yazaki, T., Ozaki, T., Tsuzuki, K., Ito, S., & Takahashi, M. (1980). Spread of varicella in hospitalized children having no direct contact with an indicator zoster case and its prevention by a live vaccine. *Biken Journal - Journal of Research Institute for Microbial Diseases*, 23, 157–61.

[5] Bahl, P., Doolan, C., de Silva, C., Chughtai, A. A., Bourouiba, L., & MacIntyre, C. R. (2020). Airborne or Droplet Precautions for Health Workers Treating Coronavirus Disease 2019? *The Journal of Infectious Diseases*, (pp. 1–8).

[6] Barberán, A., Henley, J., Fierer, N., & Casamayor, E. O. (2014). Structure, inter-annual recurrence, and global-scale connectivity of airborne microbial communities. *Science of the Total Environment*, 487(1), 187–195.

[7] Beggs, C. (2020). Is there an airborne component to the transmission of COVID-19?: a quantitative analysis study. *medRxiv*.

[8] Belov, A. A., Cheptsov, V. S., & Vorobyova, E. A. (2018). Soil bacterial communities of Sahara and Gibson deserts: Physiological and taxonomical characteristics. *AIMS Microbiology*, 4(4), 685–710.

[9] Berry, E. D., Wells, J. E., Bono, J. L., Woodbury, B. L., Kalchayanand, N., Norman, K. N., & Millner, P. D. (2015). Effect of proximity to a cattle feedlot on Escherichia coli O157:

H7 contamination of leafy greens and evaluation of the potential for airborne transmission. *Applied and Environmental Microbiology*, 81(3), 1101–1110.

[10] Bertolini, V., Gandolfi, I., Ambrosini, R., Bestetti, G., Innocente, E., Rampazzo, G., & Franzetti, A. (2013). Temporal variability and effect of environmental variables on airborne bacterial communities in an urban area of Northern Italy. *Applied Microbiology and Biotechnology*, 97(14), 6561–6570.

[11] Binder, R. A., Alarja, N. A., Robie, E. R., Kochek, K. E., Xiu, L., Rocha-Melogno, L., Abdelgadir, A., Goli, S. V., Farrell, A. S., Coleman, K. K., Turner, A. L., Lautredou, C. C., Lednicky, J. A., Lee, M. J., Polage, C. R., Simmons, R. A., Deshusses, M. A., Anderson, B. D., & Gray, G. C. (2020). Environmental and Aerosolized Severe Acute Respiratory Syndrome Coronavirus 2 Among Hospitalized Coronavirus Disease 2019 Patients. *The Journal of Infectious Diseases*, 222(11), 1798–1806.

[12] Block, S. (2001). The Growing Threat of Biological Weapons: The terrorist threat is very real, and it's about to get worse. Scientists should concern themselves before it's too late. *American Scientist*, 89(1), 28–37.

[13] Bosshard, P. P. (2000). Seasonal and spatial community dynamics. *Archives of Microbiology*, 174(3), 168–174.

[14] Botton, S., Van Heusden, M., Parsons, J., Smidt, H., & Van Straalen, N. (2006). Resilience of microbial systems towards disturbances. *Critical Reviews in Microbiology*, 32(2), 101–112.

[15] Bottone, E. J. (2010). Bacillus cereus, a volatile human pathogen. *Clinical Microbiology Reviews*, 23(2), 382–398.

[16] Bourouiba, L. (2020). Turbulent Gas Clouds and Respiratory Pathogen Emissions: Potential Implications for Reducing Transmission of COVID-19. *JAMA - Journal of the American Medical Association*, 323(18), 1837–1838.

[17] Bourouiba, L., Dehandschoewercker, E., & Bush, J. W. (2014). Violent expiratory events: on coughing and sneezing. *Journal of Fluid Mechanics*, 745, 537–563.

[18] Bowden, J., Gregory, P., & Johnson, C. (1971). Possible wind transport of coffee leaf rust across the Atlantic Ocean. *Nature*, 229(5285), 500–501.

[19] Bowers, R. M., Clements, N., Emerson, J. B., Wiedinmyer, C., Hannigan, M. P., & Fierer, N. (2013). Seasonal variability in bacterial and fungal diversity of the near-surface atmosphere. *Environmental Science and Technology*, 47(21), 12097–12106.

[20] Bowers, R. M., McLetchie, S., Knight, R., & Fierer, N. (2011a). Spatial variability in airborne bacterial communities across land-use types and their relationship to the bacterial communities of potential source environments. *The ISME Journal*, 5(4), 601–612.

[21] Bowers, R. M., Sullivan, A. P., Costello, E. K., Collett, J. L., Knight, R., & Fierer, N. (2011b). Sources of bacteria in outdoor air across cities in the midwestern United States. *Applied and Environmental Microbiology*, 77(18), 6350–6356.

[22] Brown, K., Bouhamra, W., Lamoureux, D., Evans, J., & Koutrakis., P. (2008). Characterization of Particulate Matter for Three Sites in Kuwait. *Journal of the Air and Waste Management Association*, 58(8), 994–1003.

[23] Buchwaldt, L., Morrall, R., Chongo, G., & Bernier, C. (1996). Windborne dispersal of Colletotrichum truncatum and survival in infested lentil debris. *Phytopathology*, 86(11), 1193–1198.

[24] Buonanno, G., Stabile, L., & Morawska, L. (2020). Estimation of airborne viral emission: Quanta emission rate of SARS-CoV-2 for infection risk assessment. *Environment International*, 141(May), 105794.

[25] Burrows, S. M., Elbert, W., Lawrence, M., & Poschl, U. (2009). Bacteria in the global atmosphere – Part 1 : Review and synthesis of literature data for different ecosystems. *Atmospheric Chemistry and Physics*, 9(1987), 9263–9280.

[26] Caporaso, J., Kuczynski, J., Stombaugh, J., Bittinger, K., Bushman, F., Costello, E., Fierer, N., Pena, A., Goodrich, J., Gordon, J., & Huttley, G. (2010). QIIME allows analysis of high-throughput community sequencing data. *Nature Methods*, 7(5), 335–336.

[27] Cha, S., Srinivasan, S., Jang, J. H., Lee, D., Lim, S., Kim, K. S., Jheong, W., Lee, D. W., Park, E. R., Chung, H. M., Choe, J., Kim, M. K., & Seo, T. (2017). Metagenomic analysis of airborne bacterial community and diversity in seoul, korea, during December 2014, asian dust event. *PLoS ONE*, 12(1), 1–12.

[28] Cheng, V. C. C., Wong, S. C., Chan, V. W. M., So, S. Y. C., Chen, J. H. K., Yip, C. C. Y., & To, K. K. W. (2020). Air and environmental sampling for SARS-CoV-2 around hospitalized patients with coronavirus disease 2019 (COVID-19). *Infection Control and Hospital Epidemiology*, 41(11), 1258–1265.

[29] Chia, P. Y., Coleman, K. K., Tan, Y. K., Ong, S. W. X., Gum, M., Lau, S. K., Gray, G. C., & Son, T. T. (2020). Detection of air and surface contamination by severe acute respiratory syndrome coronavirus 2 (SARS-CoV-2) in hospital rooms of infected patients. *Nature Communications*, 11(1), 1–7.

[30] Christensen, L., Mortensen, S., Bøtner, A., Strandbygaard, B., Rønsholt, L., Henriksen, C., & Andersen, J. (1993). Further evidence of long distance airborne transmission of Aujeszky's disease (pseudorabies) virus. *The Veterinary Record*, 32(13), 317–321.

[31] Chuvochina, M. S., Alekhina, I. A., Normand, P., Petit, J. R., & Bulat, S. A. (2011). Three events of Saharan dust deposition on the Mont Blanc glacier associated with different snow-colonizing bacterial phylotypes. *Microbiology*, 80, 125–131.

[32] Clark, K., Karsch-Mizrachi, I., Lipman, D. J., Ostell, J., & Sayers, E. W. (2016). GenBank. *Nucleic Acids Research*, 44(D1), D67–D72.

[33] Clements, A., Young, J. C., Constantinou, N., & Frankel, G. (2012). Infection strategies of enteric pathogenic Escherichia coli. *Gut Microbes*, 3(2), 71–87.

[34] Coronaviridae Study Group of the International Committee on Taxonomy of Viruses (2020). The species Severe acute respiratory syndrome-related coronavirus: classifying 2019-nCoV and naming it SARS-CoV-2. *Nature Microbiology*, 5(4), 536–544.

[35] D'Almeida, G. A. (1986). A model for Saharan dust transport. *Journal of Climate and Applied Meteorology*, 25(7), 903–916.

[36] De Groot, A., Chapon, V., Servant, P., Christen, R., Fischer-Le Saux, M., Sommer, S., & Heulin, T. (2005). Deinococcus deserti sp. nov., a gamma-radiation-tolerant bacterium isolated from the Sahara Desert. *International Journal of Systematic and Evolutionary Microbiology*, 55, 2441–2446.

[37] del Carmen Montero-Calasanz, M., Göker, M., Pötter, G., Rohde, M., Spröer, C., Schumann, P., & Klenk, H. P. (2013). Geodermatophilus africanus sp. nov., a halotolerant actinomycete isolated from Saharan desert sand. *Antonie Van Leeuwenhoek*, 104(2), 207–216.

[38] Delort, A.-m. & Amato, P. (2017). *Microbiology of Aerosols*. John Wiley & Sons, Inc.

[39] Demokritou, P., Gupta, T., Ferguson, S., & Koutrakis, P. (2002). Development and Laboratory Performance Evaluation of a Personal Cascade Impactor. *Journal of the Air and Waste Management Association*, 52, 1230–1237.

[40] Demokritou, P., Lee, S. J., Ferguson, S. T., & Koutrakis, P. (2004). A compact multistage (cascade) impactor for the characterization of atmospheric aerosols. *Journal of Aerosol Science*, 35(3), 281–299.

[41] DeSantis, T. Z., Hugenholtz, P., Larsen, N., Rojas, M., Brodie, E. L., Keller, K., & Andersen, G. L. (2006). Greengenes, a chimera-checked 16S rRNA gene database and workbench compatible with ARB. *Applied and Environmental Microbiology*, 72(7), 5069–5072.

[42] Ding, Z., Qian, H., Xu, B., Huang, Y., Miao, T., Yen, H.-L., Xiao, S., Cui, L., Wu, X., Shao, W., Song, Y., Sha, L., Zhou, L., Xu, Y., Zhu, B., & Li, Y. (2020). Toilets dominate environmental detection of SARS-CoV-2 virus in a hospital. *medRxiv*.

[43] Dommergue, A., Amato, P., Tignat-Perrier, R., Magand, O., Thollot, A., Joly, M., Bouvier, L., Sellegri, K., Vogel, T., Sonke, J. E., Jaffrezo, J. L., Andrade, M., Moreno, I., Labuschagne, C., Martin, L., Zhang, Q., & Larose, C. (2019). Methods to investigate the global atmospheric microbiome. *Frontiers in Microbiology*, 10(FEB), 1–12.

[44] Edgar, R. C. (2010). Search and clustering orders of magnitude faster than BLAST. *Bioinformatics*, 26(19), 2460–2461.

[45] Eilers, H., Pernthaler, J., Glöckner, F. O., & Amann, R. (2000). Culturability and in situ abundance of pelagic bacteria from the North Sea. *Applied and Environmental Microbiology*, 66(7), 3044–3051.

[46] Eppard, M., Krumbein, W. E., Koch, C., Rhiel, E., Staley, J. T., & Stackebrandt, E. (1996). Morphological, physiological, and molecular characterization of actinomycetes isolated from dry soil, rocks, and monument surfaces. *Archives of Microbiology*, 166(1), 12–22.

[47] Fahlgren, C., Bratbak, G., Sandaa, R. A., Thyrhaug, R., & Zweifel, U. L. (2011). Diversity of airborne bacteria in samples collected using different devices for aerosol collection. *Aerobiologia*, 27(2), 107–120.

[48] Faridi, S., Niazi, S., Sadeghi, K., Naddafi, K., Yavarian, J., Shamsipour, M., Jandaghi, N., Sadeghniiat, K., Nabizadeh, R., Yunesian, M., & Momeniha, F. (2020). A field indoor air measurement of SARS-CoV-2 in the patient rooms of the largest hospital in Iran. *Science of the Total Environment*, 725, 138401.

[49] Favet, J., Lapanje, A., Giongo, A., Kennedy, S., Aung, Y. Y., Cattaneo, A., Davis-Richardson, A. G., Brown, C. T., Kort, R., Brumsack, H. J., Schnetger, B., Chappell, A., Kroijenga, J., Beck, A., Schwibbert, K., Mohamed, A. H., Kirchner, T., De Quadros, P. D., Triplett, E. W., Broughton, W. J., & Gorbushina, A. A. (2013). Microbial hitchhikers on intercontinental dust: Catching a lift in Chad. *The ISME Journal*, 7(4), 850–867.

[50] Fears, A., Klimstra, W., Duprex, P., Hartman, A., Weaver, S., Plante, K., Mirchandani, D., Plante, J., Aguilar, P., Fernandez, D., Nalca, A., Totura, A., Dyer, D., Kearney, B., Lackemeyer, M., Bohannon, J. K., Johnson, R., Garry, R., Reed, D., & Roy, C. (2020). Comparative dynamic aerosol efficiencies of three emergent coronaviruses and the unusual persistence of SARS-CoV-2 in aerosol suspensions. *medRxiv*, 2.

[51] Fernandez-Montero, J. V., Soriano, V., Barreiro, P., de Mendoza, C., & Artacho, M. Á. (2020). Coronavirus and other airborne agents with pandemic potential. *Current Opinion in Environmental Science & Health*, 17, 41–48.

[52] Fierer, N., Leff, J. W., Adams, B. J., Nielsen, U. N., Bates, S. T., & Lauber, C. L. (2012). Cross-biome metagenomic analyses of soil microbial communities and their functional attributes. *Proceedings of the National Academy of Sciences*, 109, 21390–21395.

[53] Fierer, N., Liu, Z., Rodríguez-Hernández, M., Knight, R., Henn, M., & Hernandez, M. T. (2008). Short-term temporal variability in airborne bacterial and fungal populations. *Applied and Environmental Microbiology*, 74(1), 200–207.

[54] Fineberg, H. (2020). *Rapid expert consultation on the possibility of bioaerosol spread of SARS-CoV-2 for the COVID-19 pandemic*. Washington, D.C.: National Academies Press (US).

[55] Franzetti, A., Gandolfi, I., Gaspari, E., Ambrosini, R., & Bestetti, G. (2011). Seasonal variability of bacteria in fine and coarse urban air particulate matter. *Applied Microbiology and Biotechnology*, 90(2), 745–753.

[56] Garrison, V., Shinn, E., Foreman, W., Griffin, D., Holmes, C., Kellogg, C., Majewski, M., Richardson, L., Ritchie, K., & Smith, G. (2003). African and Asian Dust: From Desert Soils to Coral Reefs. *BioScience*, 53(5), 469.

[57] Gillies, J. A., Nickling, W. G., & McTainsh, G. H. (1996). Dust concentrations and particle-size characteristics of an intense dust haze event: Inland Delta region, Mali, West Africa. *Atmospheric Environment*, 30(7), 1081–1090.

[58] Giongo, A., Favet, J., Lapanje, A., Gano, K. A., Kennedy, S., Davis-Richardson, A. G., Brown, C., Beck, A., Farmerie, W. G., Cattaneo, A., Crabb, D. B., Aung, Y. Y., Kort, R., Brumsack, H. J., Schnetger, B., Broughton, W. J., Gorbushina, A. A., & Triplett, E. W. (2013). Microbial hitchhikers on intercontinental dust: High-throughput sequencing to catalogue microbes in small sand samples. *Aerobiologia*, 29(1), 71–84.

[59] González-Toril, E., Osuna, S., Viúdez-Moreiras, D., Navarro-Cid, I., del Toro, S. D., Sor, S., & Aguilera, A. (2020). Impacts of Saharan Dust intrusions on Bacterial communities of the Low troposphere. *Scientific Reports*, 10(1), 1–13.

[60] Good, J. (1953). The Population Frequencies of Species and the Estimation of Population Parameters. *Biometrika*, 40(3/4), 237–264.

[61] Gorbushina, A. A., Kort, R., Schulte, A., Lazarus, D., Schnetger, B., Brumsack, H. J., Broughton, W. J., & Favet, J. (2007). Life in Darwin's dust: Intercontinental transport and survival of microbes in the nineteenth century. *Environmental Microbiology*, 9(12), 2911–2922.

[62] Gregory, P. H. (1971). The Leeuwenhoek Lecture 1970 Airborne microbes: their significance and distribution. *Proceedings of the Royal Society of London. Series B. Biological Sciences*, 177(1049), 469–483.

[63] Griffin, D., Kellogg, C., & Shinn, E. (2001a). Dust in the Wind: Long Range Transport of Dust in the Atmosphere and Its Implications for Global Public and Ecosystem Health. *Global Change and Human Health*, 2(1), 20–33.

[64] Griffin, D. W. (2007). Atmospheric movement of microorganisms in clouds of desert dust and implications for human health. *Clinical Microbiology Reviews*, 20(3), 459–477.

[65] Griffin, D. W., Garrison, V. H., Herman, J. R., & Shinn, E. A. (2001b). African desert dust in the Caribbean atmosphere: Microbiology and public health. *Aerobiologia*, 17(3), 203–213.

[66] Hadfield, J., Megill, C., Bell, S. M., Huddleston, J., Potter, B., Callender, C., & Neher, R. A. (2018). Nextstrain: real-time tracking of pathogen evolution. *Bioinformatics*, 34(23), 4121–4123.

[67] Hamner, L., Dubbel, P., & Capron, I. (2020). High SARS-CoV-2 attack rate following exposure at a choir practice - Skagit County, Washington, March 2020. *Morbidity and Mortality Weekly Report*, 69, 606–10.

[68] Hanada, S. & Sekiguchi, Y. (2014). The phylum gemmatimonadetes. In E. Rosenberg, E. Delong, S. Lory, E. Stackebrandt, & F. Thompson (Eds.), *The Prokaryotes* (pp. 677–681). New York: Springer.

[69] Heidelberg, J. F., Shahamat, M., Levin, M., Rahman, I., Stelma, G., Grim, C., & Colwell, R. R. (1997). Effect of aerosolization on culturability and viability of gram-negative bacteria. *Applied and Environmental Microbiology*, 63(9), 3585–3588.

[70] Hervas, A. & Casamayor, E. O. (2009). High similarity between bacterioneuston and airborne bacterial community compositions in a high mountain lake area. *FEMS Microbiology Ecology*, 67(2), 219–228.

[71] Hinds, W. (2012). *Aerosol Technology: Properties, Behavior, and Measurement of Airborne Particles*. John Wiley & Sons.

[72] Houghton, K., Morgan, X., Lagutin, K., MacKenzie, A., Vyssotskii, M., Mitchell, K., McDonald, I., Morgan, H., Power, J., Moreau, J., Hanssen, E., & Stott, M. (2015). Thermorudis pharmacophila sp. nov., a novel member of the class Thermomicrobia isolated from geothermal soil, and emended descriptions of Thermomicrobium roseum, Thermomicrobium carboxidum, Thermorudis peleae and Sphaerobacter thermophil. *International Journal of Systematic and Evolutionary Microbiology*, 65(12), 4479–87.

[73] Ivanova, N., Sikorski, J., Jando, M., Munk, C., Lapidus, A., Del Rio, T. G., & Chen, F. (2010). Complete genome sequence of Geodermatophilus obscurus type strain (G-20 T). *Standards in Genomic Sciences*, 2(2), 158–167.

[74] Jacob, D. (1999). Aerosols. In *Introduction to Atmospheric Chemistry* (pp. 144–153). Princeton University Press.

[75] Jaenicke, R. (2005). Abundance of cellular material and proteins in the atmosphere. *Science*, 308(5718), 73.

[76] Jeon, E. M., Kim, H. J., Jung, K., Kim, J. H., Kim, M. Y., Kim, Y. P., & Ka, J. O. (2011). Impact of Asian dust events on airborne bacterial community assessed by molecular analyses. *Atmospheric Environment*, 45(25), 4313–4321.

[77] Johnson, G. R., Morawska, L., Ristovski, Z. D., Hargreaves, M., Mengersen, K., Chao, C. Y. H., & Corbett, S. (2011). Modality of human expired aerosol size distributions. *Journal of Aerosol Science*, 42(12), 839–851.

[78] Katra, I., Arotsker, L., Krasnov, H., Zaritsky, A., Kushmaro, A., & Ben-Dov, E. (2014). Richness and diversity in dust stormborne biomes at the southeast mediterranean. *Scientific Reports*, 4, 19–24.

[79] Kavouras, I. G. & Koutrakis, P. (2001). Use of Polyurethane Foam as the Impaction Substrate/Collection Medium in Conventional Inertial Impactors. *Aerosol Science and Technology*, 34(1), 46–56.

[80] Kellogg, C. A. & Griffin, D. W. (2006). Aerobiology and the global transport of desert dust. *Trends in Ecology & Evolution*, 21(11), 638–644.

[81] Kellogg, C. A., Griffin, D. W., Garrison, V. H., Peak, K. K., Royall, N., Smith, R. R., & Shinn, E. A. (2004). Characterization of aerosolized bacteria and fungi from desert dust events in Mali, West Africa. *Aerobiologia*, 20(2), 99–110.

[82] Kenarkoohi, A., Noorimotlagh, Z., Falahi, S., Amarloei, A., Mirzaee, S. A., Pakzad, I., & Bastani, E. (2020). Hospital indoor air quality monitoring for the detection of SARS-CoV-2 (COVID-19) virus. *Science of the Total Environment*, 748, 141324.

[83] Klein, A. M., Bohannan, B. J., Jaffe, D. A., Levin, D. A., & Green, J. L. (2016). Molecular evidence for metabolically active bacteria in the atmosphere. *Frontiers in Microbiology*, 7(MAY), 1–11.

[84] Lednicky, J. A., Lauzard, M., Fan, Z. H., Jutla, A., Tilly, T. B., Gangwar, M., Usmani, M., Shankar, S. N., Mohamed, K., Eiguren-Fernandez, A., Stephenson, C. J., Alam, M. M., Elbadry, M. A., Loeb, J. C., Subramaniam, K., Waltzek, T. B., Cherabuddi, K., Morris, J. G., & Wu, C. Y. (2020). Viable SARS-CoV-2 in the air of a hospital room with COVID-19 patients. *International Journal of Infectious Diseases*, 100, 476–482.

[85] Lednicky, J. A., Lauzardo, M., Alam, M. M., Elbadry, M., Stephenson, C., Gibson, J. C., & Morris, J. G. (2021). Isolation of SARS-CoV-2 from the air in a car driven by a COVID patient with mild illness. *medRxiv*.

[86] Lee, J. K. & Jeong, H. W. (2020). Rapid expansion of temporary, reliable airborne-infection isolation rooms with negative air machines for critical COVID-19 patients. *American Journal of Infection Control*, 48(7), 822–824.

[87] Lemieux, J., Siddle, K., Shaw, B., Loreth, C., ..., & MacInnis, B. (2020). Phylogenetic analysis of SARS-CoV-2 in the Boston area highlights the role of recurrent importation and super-spreading events. *medRxiv*.

[88] Levetin, E. (2007). Aerobiology of agricultural pathogens. In *Manual of Environmental Microbiology, Third Edition* (pp. 1031–1047). American Society of Microbiology.

[89] Li, Y. H., Fan, Y. Z., Jiang, L., & Wang, H. B. (2020). Aerosol and environmental surface monitoring for SARS-CoV-2 RNA in a designated hospital for severe COVID-19 patients. *Epidemiology and Infection*, 148(e154), 1–5.

[90] Lighthart, B. & Shaffer, B. T. (1995). Airborne bacteria in the atmospheric surface layer: Temporal distribution above a grass seed field. *Applied and Environmental Microbiology*, 61(4), 1492–1496.

[91] Liu, C., Yang, J., Ji, S., Lu, Y., Wu, P., & Chen, C. (2018). Influence of natural ventilation rate on indoor PM2. 5 deposition. *Building and Environment*, 144, 357–364.

[92] Liu, Y., Ning, Z., Chen, Y., Guo, M., Liu, Y., Gali, N. K., Sun, L., Duan, Y., Cai, J., Westerdahl, D., Liu, X., Xu, K., fai Ho, K., Kan, H., Fu, Q., & Lan, K. (2020). Aerodynamic analysis of SARS-CoV-2 in two Wuhan hospitals. *Nature*, 582(7813), 557–560.

[93] Locey, K. J. & Lennon, J. T. (2016). Scaling laws predict global microbial diversity. *Proceedings of the National Academy of Sciences*, 113(21), 5970–5975.

[94] Lozupone, C. & Knight, R. (2005). UniFrac: A new phylogenetic method for comparing microbial communities. *Applied and Environmental Microbiology*, 71(12), 8228–8235.

[95] Lu, R., Li, Y., Li, W., Xie, Z., Fan, C., Liu, P., & Deng, S. (2018). Bacterial community structure in atmospheric particulate matters of different sizes during the haze days in Xi'an, China. *Science of the Total Environment*, 637-638, 244–252.

[96] Ma, J., Qi, X., Chen, H., Li, X., Zhang, Z., Wang, H., Sun, L., Zhang, L., Guo, J., Morawska, L., & Grinshpun, S. (2020). Coronavirus Disease 2019 Patients in Earlier Stages Exhaled Millions of Severe Acute Respiratory Syndrome Coronavirus 2 Per Hour. *Clinical Infectious Diseases*, Brief Report.

[97] Mahmoudi, N., Beaupré, S. R., Steen, A. D., & Pearson, A. (2017). Sequential bioavailability of sedimentary organic matter to heterotrophic bacteria. *Environmental Microbiology*, 19(7), 2629–2644.

[98] Marple, V. A. & Liu, B. H. (1974). Characteristics of Laminar Jet Impactors. *Environmental Science and Technology*, 8, 648–654.

[99] Masoumbeigi, H., Ghanizadeh, G., Arfaei, R., Heydari, S., Goodarzi, H., Sari, R., & Tat, M. (2020). Investigation of hospital indoor air quality for the presence of SARS-Cov-2. *Journal of Environmental Health Science and Engineering*, 18(2), 1259–1263.

[100] Masri, S., Kang, C. M., & Koutrakis, P. (2015). Composition and sources of fine and coarse particles collected during 2002–2010 in Boston, MA. *Journal of the Air & Waste Management Association*, 65(3), 287–297.

[101] Mazar, Y., Cytryn, E., Erel, Y., & Rudich, Y. (2016). Effect of Dust Storms on the Atmospheric Microbiome in the Eastern Mediterranean. *Environmental Science and Technology*, 50(8), 4194–4202.

[102] McDonald, D., Price, M. N., Goodrich, J., Nawrocki, E. P., Desantis, T. Z., Probst, A., Andersen, G. L., Knight, R., & Hugenholtz, P. (2012). An improved Greengenes taxonomy with explicit ranks for ecological and evolutionary analyses of bacteria and archaea. *The ISME Journal*, 6(3), 610–618.

[103] McMurdie, P. J. & Holmes, S. (2013). Phyloseq: An R Package for Reproducible Interactive Analysis and Graphics of Microbiome Census Data. *PLoS ONE*, 8(4), e61217.

[104] Meola, M., Lazzaro, A., & Zeyer, J. (2015). Bacterial composition and survival on Sahara dust particles transported to the European Alps. *Frontiers in Microbiology*, 6(DEC), 1–17.

[105] Middleton, N. J. & Goudie, A. S. (2001). Saharan dust: Sources and trajectories. *Transactions of the Institute of British Geographers*, 26(2), 165–181.

[106] Mikkelsen, T., Alexandersen, S., Astrup, P., Champion, H. J., Donaldson, A. I., Dunkerley, F. N., Gloster, J., Sørensen, J. H., & Thykier-Nielsen, S. (2003). Investigation of airborne foot-and-mouth disease virus transmission during low-wind conditions in the early phase of the UK 2001 epidemic. *Atmospheric Chemistry and Physics*, 3(6), 2101–2110.

[107] Morawska, L. & Cao, J. (2020). Airborne transmission of SARS-CoV-2: The world should face the reality. *Environment International*, 139(April), 105730.

[108] Morawska, L. & Milton, D. (2020). It Is Time to Address Airborne Transmission of Coronavirus Disease 2019 (COVID-19). *Clinical Infectious Diseases*, 71(9), 2311–2313.

[109] Morris, C. E., Sands, D. C., Bardin, M., Jaenicke, R., Vogel, B., Leyronas, C., Ariya, P. A., & Psenner, R. (2011). Microbiology and atmospheric processes: Research challenges concerning the impact of airborne micro-organisms on the atmosphere and climate. *Biogeosciences*, 8(1), 17–25.

[110] Moulin, C., Lambert, C. E., Dulac, F., & Dayan, U. (1997). Control of atmospheric export of dust from North Africa by the North Atlantic Oscillation. *Nature*, 387(6634), 691–694.

[111] Navas-Molina, J., Peralta-Sánchez, J., González, A., McMurdie, P., Vázquez-Baeza, Y., Xu, Z., Ursell, L., Lauber, C., Zhou, H., Song, S., & Huntley, J. (2013). Advancing our understanding of the human microbiome using QIIME. *Methods in Enzymology*, 531, 371–444.

[112] Nicas, M., Nazaroff, W., & Hubbard, A. (2005). Toward understanding the risk of secondary airborne infection: emission of respirable pathogens. *Journal of Occupational and Environmental Hygiene*, 2(3), 143–154.

[113] Nishiura, H., Oshitani, H., Kobayashi, T., Saito, T., Sunagawa, T., Matsui, T., Wakita, T., & Suzuki, M. (2020). Closed environments facilitate secondary transmission of coronavirus disease 2019 (COVID-19). *medRxiv*.

[114] Noorimotlagh, Z., Jaafarzadeh, N., Martínez, S. S., & Mirzaee, S. A. (2020). A systematic review of possible airborne transmission of the COVID-19 virus (SARS-CoV-2) in the indoor air environment. *Environmental Research*, 110612.

[115] Oksanen, J., Kindt, R., Legendre, P., O'Hara, B., Simpson, G. L., Solymos, P., Stevens, M. H. H., & Wagner, H. (2008). *vegan: Community Ecology Package*. R package version 1.15-1.

[116] Ong, S. W. X., Tan, Y. K., Chia, P. Y., Lee, T. H., Ng, O. T., Wong, M. S. Y., & Marimuthu, K. (2020). Air, Surface Environmental, and Personal Protective Equipment Contamination by Severe Acute Respiratory Syndrome Coronavirus 2 (SARS-CoV-2) from a Symptomatic Patient. *Journal of the American Medical Association*, 323(16), 1610–1612.

[117] Ott, L. (2018). Adhesion properties of toxigenic corynebacteria. *AIMS microbiology*, 4(1), 85.

[118] Papineni, R. S. & Rosenthal, F. S. (1997). The size distribution of droplets in the exhaled breath of healthy human subjects. *Journal of Aerosol Medicine*, 10(2), 105–116.

[119] Parada, A. E., Needham, D. M., & Fuhrman, J. A. (2016). Every base matters: assessing small subunit rRNA primers for marine microbiomes with mock communities, time series and global field samples. *Environmental Microbiology*, 18(5), 1403–1414.

[120] Park, S., Kim, Y., & Yi, S. (2020). Coronavirus disease outbreak in call center, South Korea. *Emerging Infectious Diseases*, 26(8), 1666.

[121] Pedgley, D. E. (1986). Long distance transport of spores. *Plant Disease Epidemiology*, 1, 346–365.

[122] Polymenakou, P. N. (2012). Atmosphere: A source of pathogenic or beneficial microbes? *Atmosphere*, 3(1), 87–102.

[123] Polymenakou, P. N., Mandalakis, M., Stephanou, E. G., & Tselepides, A. (2008). Particle size distribution of airborne microorganisms and pathogens during an intense African dust event in the eastern Mediterranean. *Environmental Health Perspectives*, 116(3), 292–296.

[124] Prospero, J. M. (1999). Long-range transport of mineral dust in the global atmosphere: Impact of African dust on the environment of the southeastern United States. *Proceedings of the National Academy of Sciences of the United States of America*, 96(7), 3396–3403.

[125] Prussin, A. J., Il, E. B. G., & Marr, L. C. (2015). Total virus and bacteria concentrations in indoor and outdoor air. *Environmental Science and Technology Letters*, 2(4), 84.

[126] Prussin, A. J. & Marr, L. C. (2015). Sources of airborne microorganisms in the built environment. *Microbiome*, 3, 78.

[127] Qian, H., Miao, T., Liu, L., Zheng, X., Luo, D., & Li, Y. (2020). Indoor transmission of SARS-CoV-2. *Indoor Air*, 00, 1–7.

[128] R Core Team (2018). *R: A Language and Environment for Statistical Computing*. R Foundation for Statistical Computing, Vienna, Austria.

[129] Razzini, K., Castrica, M., Menchetti, L., Maggi, L., Negroni, L., Orfeo, N. V., Pizzoccheri, A., Stocco, M., Muttini, S., & Balzaretti, C. M. (2020). SARS-CoV-2 RNA detection in the air and on surfaces in the COVID-19 ward of a hospital in Milan, Italy. *Science of the Total Environment*, 742, 140540.

[130] Reiner Jr, R. C., Graetz, N., Casey, D. C., Troeger, C., Garcia, G. M., Mosser, J. F., & Rao, P. C. (2018). Variation in childhood diarrheal morbidity and mortality in Africa, 2000–2015. *New England Journal of Medicine*, 379(12), 1128–1138.

[131] Remington, P., Hall, W., Davis, I., Herald, A., & Gunn, R. (1985). Airborne transmission of measles in a physician's office. *JAMA - Journal of the American Medical Association*, 253, 1574–7.

[132] Rhee, C., Baker, M., Vaidya, V., Tucker, R., Resnick, A., Morris, C. A., & CDC Prevention Epicenters Program (2020). Incidence of nosocomial COVID-19 in patients hospitalized at a large US academic medical center. *JAMA Network Open*, 3(9), e2020498–e2020498.

[133] Riley, R., Mills, C., Nyka, W., Weinstock, N., Story, P., Sultan, L., Riley, M., & Wells, W. (1959). Aerial Dissemination of pulmonary tuberculosis a two year study of contagion in a tuberculosis ward. *American Journal of Hygiene*, 70, 185–196.

[134] Ruzer, L. S. & Harley, N. H., Eds. (2013). *Aerosols Handbook: Measurement, Dosimetry, and Health Effects, Second Edition*. Boca Raton: CRC Press.

[135] Sadikot, R. T., Blackwell, T. S., Christman, J. W., & Prince, A. S. (2005). Pathogen–host interactions in Pseudomonas aeruginosa pneumonia. *American Journal of Respiratory and Critical Care Medicine*, 171(11), 1209–1223.

[136] Sanchez de la Camp, A., Garcia-Salamanca, A., Solano, J., de la Rosa, J., & Ramos, J.-L. (2013). Chemical and Microbiological Characterization of Atmospheric Particulate Matter during an Intense African Dust Event in Southern Spain. *Environmental Science and Technology*, 47, 3630–3638.

[137] Santarpia, J. L., Herrera, V. L., Rivera, D. N., Ratnesar-Shumate, S., Denton, P. W., Martens, J. W., & Brett-Major, D. M. (2020a). The infectious nature of patient-generated SARS-CoV-2 aerosol. *MedRxiv*.

[138] Santarpia, J. L., Rivera, D. N., Herrera, V. L., Morwitzer, M. J., Creager, H. M., Santarpia, G. W., Crown, K. K., Brett-Major, D. M., Schnaubelt, E. R., Broadhurst, M. J., Lawler, J. V., Reid, S. P., & Lowe, J. J. (2020b). Aerosol and surface contamination of SARS-CoV-2 observed in quarantine and isolation care. *Scientific Reports*, 10(1), 3–5.

[139] Shao, Y., Klose, M., & Wyrwoll, K. H. (2013). Recent global dust trend and connections to climate forcing. *Journal of Geophysical Research Atmospheres*, 118(19), 11107–11118.

[140] Siegel, J., Rhinehart, E., Jackson, M., & Chiarello, L. (2007). Health Care Infection Control Practices Advisory Committee 2007 guideline for isolation precautions: preventing transmission of infectious agents in health care settings. *American Journal of Infection Control*, 35 (10 Sup, S65–164.

[141] Smith, P., Anderson, A., & Christohper, G. (2006). Designing a biocontainment unit to care for patients with serious communicable diseases: a consensus statement. *Biosecurity and Bioterrorism: Biodefense Strategy, Practice, and Science*, 4, 351–365.

[142] Smither, S. J., Eastaugh, L. S., Findlay, J. S., & Lever, M. S. (2020). Experimental aerosol survival of SARS-CoV-2 in artificial saliva and tissue culture media at medium and high humidity. *Emerging Microbes & Infections*, 9(1), 1415–1417.

[143] Stadnytskyi, V., Bax, C., Bax, A., & Anfinrud, P. (2020). The airborne lifetime of small speech droplets and their potential importance in SARS-CoV-2 transmission. *Proceedings of the National Academy of Sciences*, 117(22), 11875–11877.

[144] Stein, A. F., Draxler, R. R., Rolph, G. D., Stunder, B. J., Cohen, M. D., & Ngan, F. (2015). NOAA's HYSPLIT atmospheric transport and dispersion modeling system. *Bulletin of the American Meteorological Society*, 96(12), 2059–2077.

[145] Stern, R., Al-Hemoud, A., Alahmad, B., & Koutrakis, P. (2021a). Levels and particle size distribution of airborne SARS-CoV-2 at a healthcare facility in Kuwait. *Science of The Total Environment*, 782, 146799.

[146] Stern, R., Koutrakis, P., Martins, M., Lemos, B., Dowd, S., Sunderland, E., & Garshick, E. (2021b). Characterization of hospital airborne SARS-CoV-2. *Respiratory Research*, 22, 73.

[147] Stern, R., Mahmoudi, N., Buckee, C., Schartup, A., Koutrakis, P., Ferguson, S., Wolfson, J., Wofsy, S., Daube, B., & Sunderland, E. (2021c). The Microbiome of Size-Fractionated Airborne Particles from the Sahara Region. *Environmental Science & Technology*, 55(3), 1487–1496.

[148] Tellier, R. (2006). Review of aerosol transmission of influenza A virus. *Emerging Infectious Diseases*, 12(11), 1657.

[149] Thomas, N. & Nigam, S. (2018). Twentieth-century climate change over Africa: Seasonal hydroclimate trends and sahara desert expansion. *Journal of Climate*, 31(9), 3349–3370.

[150] Thomas, R. J. (2013). Particle size and pathogenicity in the respiratory tract. *Virulence*, 4(8), 847–858.

[151] Toepfer, I., Favet, J., Schulte, A., Schmölling, M., Butte, W., Triplett, E. W., Broughton, W. J., & Gorbushina, A. A. (2012). Pathogens as potential hitchhikers on intercontinental dust. *Aerobiologia*, 28(2), 221–231.

[152] Tong, Y. Y. & Lighthart, B. (1997). Solar radiation is shown to select for pigmented bacteria in the ambient outdoor atmosphere. *Photochemistry and Photobiology*, 65, 103–106.

[153] Torsvik, V., Goksøyr, J., & Daae, F. L. (1990). High diversity in DNA of soil bacteria. *Applied and Environmental Microbiology*, 56(3), 782–787.

[154] Trunk, T., Khalil, H. S., & Leo, J. C. (2018). Bacterial autoaggregation. *AIMS microbiology*, 4(1), 140.

[155] US Centers for Disease Control and Prevention (2020). 2019-Novel Coronavirus (2019-nCoV) Real-time rRT-PCR Panel Primers and Probes. https://www.cdc.gov/coronavirus/2019-ncov/downloads/rt-pcr-panel-primer-probes.pdf.

[156] U.S. Department of Labor (2020). Healthcare Workers and Employers. https://www.osha.gov/SLTC/covid-19/healthcare-workers.html.

[157] Van Doremalen, N., Bushmaker, T., Morris, D. H., Holbrook, M. G., Gamble, A., Williamson, B. N., Tamin, A., Harcourt, J. L., Thornburg, N. J., Gerber, S. I., Lloyd-Smith, J. O., De Wit, E., & Munster, V. J. (2020). Aerosol and surface stability of SARS-CoV-2 as compared with SARS-CoV-1. *New England Journal of Medicine*, 382(16), 1564–1567.

[158] Venkatesh, M., Joshi, K., Harjai, S., & Ramdeo, I. (1975). Aspergillosis in desert locust (Schistocerka gregaria Forsk). *Mycopathologia*, 57(3), 135–138.

[159] Wan, G. H., Wu, C. L., Chen, Y. F., Huang, S. H., Wang, Y. L., & Chen, C. W. (2014). Particle size concentration distribution and influences on exhaled breath particles in mechanically ventilated patients. *PloS one*, 9(1), e87088.

[160] Wang, J. & Du, G. (2020). COVID-19 may transmit through aerosol. *Irish Journal of Medical Science*, 24, 1–2.

[161] Wang, J. D. & Levin, P. (2009). Metabolism, cell growth and the bacterial cell cycle. *Nature Reviews Microbiology*, 7(11), 822–827.

[162] Wang, Q., Garrity, G. M., Tiedje, J. M., & Cole, J. R. (2007). Naïve Bayesian classifier for rapid assignment of rRNA sequences into the new bacterial taxonomy. *Applied and Environmental Microbiology*, 73(16), 5261–5267.

[163] Watanabe, T., Bartrand, T. A., Weir, M. H., Omura, T., & Haas, C. N. (2010). Development of a dose-response model for SARS coronavirus. *Risk Analysis*, 30(7), 1129–1138.

[164] Weissman, D. N., De Perio, M. A., & Radonovich, L. J. (2020). COVID-19 and risks posed to personnel during endotracheal intubation. *JAMA - Journal of the American Medical Association*, 323(20), 2027–2028.

[165] Wells, W. F. (1934). On air-borne infection. Study II. Droplets and droplet nuclei. *American Journal of Hygiene*, 20, 611–618.

[166] Werner, J. J., Koren, O., Hugenholtz, P., Desantis, T. Z., Walters, W. A., Caporaso, J. G., Angenent, L. T., Knight, R., & Ley, R. E. (2012). Impact of training sets on classification of high-throughput bacterial 16s rRNA gene surveys. *The ISME Journal*, 6(1), 94–103.

[167] Wölfel, R., Corman, V. M., Guggemos, W., Seilmaier, M., Zange, S., Müller, M. A., & Hoelscher, M. (2020). Virological assessment of hospitalized patients with COVID-2019. *Nature*, 581(7809), 465–469.

[168] Wooster, G. & Bowser, P. (1996). The aerobiological pathway of a fish pathogen: survival and dissemination of Aeromonas salmonicida in aerosols and its implications in fish health management. *Journal of the World Aquaculture Society*, 27(1), 7–14.

[169] World Health Organization (2014). Infection Prevention and Control of Epidemic- and Pandemic-Prone Acute Respiratory Infections in Health Care. https://www.who.int/publications/i/item/infection-prevention-and-control-\of-epidemic-and-pandemic-prone-acute-respiratory-infections-in-health-care.

[170] World Health Organization (2020). *Overview of public health and social measures in the context of COVID-19: Interim Guidance*. Technical report, World Health Organization.

[171] Xie, W., Fan, Y., Zhang, X., Tian, G., & Si, P. (2020). A mathematical model for predicting indoor PM2. 5 concentration under different ventilation methods in residential buildings. *Building Services Engineering Research and Technology*, 41(6), 694–708.

[172] Yamaguchi, N., Ichijo, T., Sakotani, A., Baba, T., & Nasu, M. (2012). Global dispersion of bacterial cells on Asian dust. *Scientific Reports*, 2(November 2010), 1–6.

[173] Yang, S., Lee, G. W., Chen, C. M., Wu, C. C., & Yu, K. P. (2007). The size and concentration of droplets generated by coughing in human subjects. *Journal of Aerosol Medicine*, 20(4), 484–494.

[174] Zhen, Q., Deng, Y., Wang, Y., Wang, X., Zhang, H., Sun, X., & Ouyang, Z. (2017). Meteorological factors had more impact on airborne bacterial communities than air pollutants. *Science of the Total Environment*, 601, 703–712.

[175] Zuo, M., Huang, Y., Ma, W., Xue, Z., Zhang, J., Gong, Y., & Che, L. (2020). Expert Recommendations for Tracheal Intubation in Critically III Patients with Noval Coronavirus Disease 2019. *Chinese Medical Sciences Journal*, 35(2), 105–109.

This thesis was typeset using LaTeX, originally developed by Leslie Lamport and based on Donald Knuth's TeX. The body text is set in 11 point Egenolff-Berner Garamond, a revival of Claude Garamont's humanist typeface. A template that can be used to format a PhD thesis with this look and feel has been released under the permissive MIT (X11) license, and can be found online at github.com/suchow/Dissertate or from its author, Jordan Suchow, at suchow@post.harvard.edu.